Analysis of Shear Strength Variance of PH 15-7 Mo Blind Rivet Stems for Aerospace Applications

A Senior Project
presented to
the Faculty of Materials Engineering
California Polytechnic State University, San Luis Obispo

In Partial Fulfillment
of the Requirements for the Degree
Bachelor of Science

Presented by
Miles MacArthur
and KC Majewski
June 2015

CHERRY®
AEROSPACE
A PCC Company

Table of Contents

1. Abstract

This project attempts to reduce manufacturing costs incurred to Cherry Aerospace by variance in material properties. To track and predict the shear strength of PH 15-7 Mo stainless steel rivet stems throughout the heat treatment process, samples were taken from several steps in the manufacturing process and experimental heat treatments were performed across a range of temperatures. The supplied rivet stems were heat treated for four hours at temperatures from 520°C to 560°C, in increments of 10°C. Double shear testing in accordance with ASTM 1312-13A revealed that there is no apparent correlation between the strength of the supplied wire and final shear strength of the wire. It is recommended that samples be tested for impact toughness to better understand the shear behavior of the rivet stem due to the break notch. When examining the effects of composition on mechanical properties, there is a lack of evidence to suggest that any correlation can be made. Even with constant composition, different lots of wire exhibit variances in shear strength in the fully heat treated condition. It is concluded that the variances in mechanical properties of the rivet stems are influenced by other factors. These could include manufacturing operations that are not included in the scope of this project, such as stackup of tolerances in the rivet assembly or effects of cold work of the wire prior to procurement by Cherry Aerospace.

Keywords: PH 15-7 Mo, Blind Rivet Stems, Shear Strength, Aerospace, Materials Engineering

2. Acknowledgements

We would like to thank Rachel Bethancourt and Caleb Lemler from Cherry Aerospace (Santa Ana, CA) for sponsoring and supporting our senior project. We would also like to thank Mr. Victor Granados and Dr. Kathy Chen for their guidance throughout the course of our project.

3. List of Figures

4. List of Tables

5. Introduction

5.1 Problem Statement

Cherry Aerospace manufactures a CherryMax blind rivet made of PH 15-7 Mo that has inconsistent shear test results. Cherry Aerospace is interested in determining the correct heat treatment based on incoming condition of raw material in order to control final shear strength. This involves a correlation between incoming shear strength of PH 15-7 stainless steel wire and a modification of the standard heat treatment to control shear strength of final product. An ideal deliverable would be a formula where shear strength of raw material is input and the adjustment to time or temperature is calculated.

5.2 General Background

Stainless steel is a category including any of several steels containing 12–30% chromium as the principal alloying element. It has gained popularity in aerospace, automotive, and construction industries because of its strength, durability, and good corrosion resistance. The specific steel under investigation is PH 15-7 Mo, that is, stainless steel containing 15% Chromium, 7% Nickel, small amounts of added Molybdenum, and that is precipitation hardened to increase strength [1]. This review highlights the specific use of PH 15-7 Mo in CherryMAX® blind rivet aerospace applications, commonly used heat treatment operations, microstructural changes in the stainless alloy, and the theories that support the observed changes.

This investigation is focused on a type of fastener used by Cherry Aerospace called a CherryMAX® blind rivet- a fastener which is used in areas where there is restricted access, or no access, to the backside of a structure. The blind rivets that are under investigation are pull-type blind fasteners, which form a “head” (sometimes called a “bulb”) on the backside of the joint using a pure pulling action [2]. As seen in Figure 1, the blind rivet is composed of four major components: the serrated stem with a break notch and grip (1), a driving anvil (or “washer”) to ensure a visible lock (2), a locking collar that mechanically locks the rivet sleeve in place (3), and a rivet sleeve (4). Figure 2 depicts the deformed rivet sleeve, the collar locked in position, and the anvil and stem sheared off. [3]

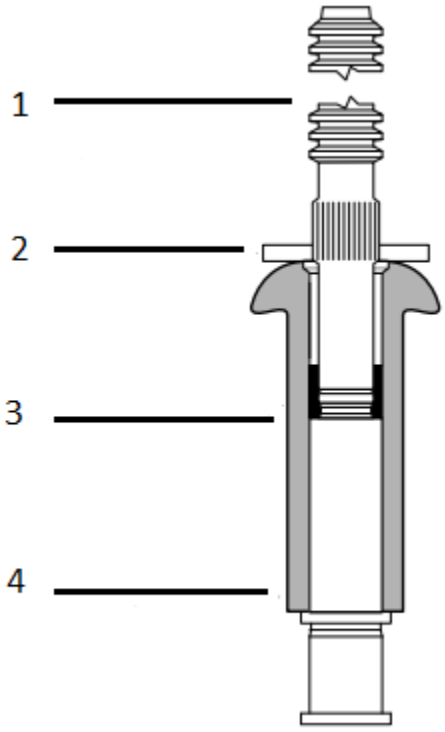

Figure 1. The four major components of a blind rivet deform and/or shear to form a solid connection. [3]

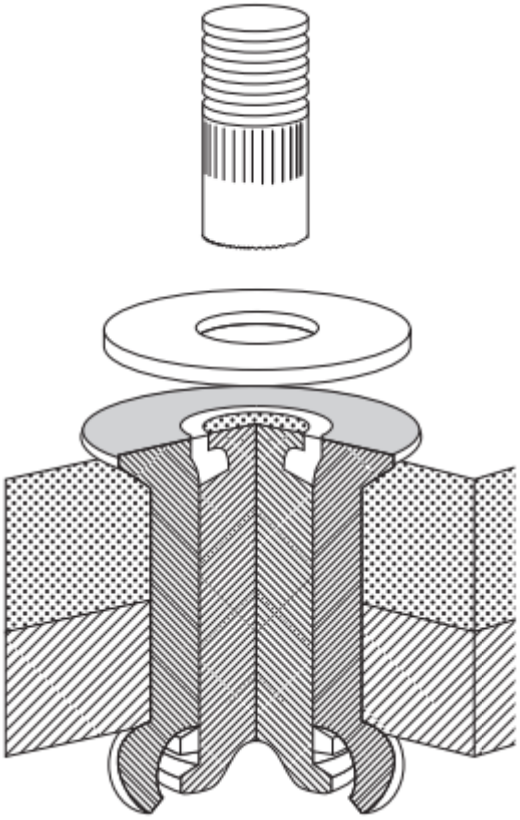

Figure 2. A cross sectional view of an installed blind rivet. [3]

The stem of the blind rivet is formed from round wire that falls into a special class of stainless steel wire called *cold-heading wire*. Cold-heading wire is manufactured with a closely controlled annealing treatment that produces optimal softness, so that the wire can be additionally cold-worked to the desired shape and mechanical properties [4]. For the specific blind rivet under investigation, the PH 15-7 Mo wire is required to have yield strength (.2% offset) of 105-125 ksi, as required by Cherry Aerospace from their suppliers of as-received wire. This range is specified because too low of a yield strength causes wire to buckle during stem heading, while too high of a yield strength causes the tooling to wear at a faster rate. It is acceptable for the material to be supplied in the *intermediate temper condition*- meaning it has been cold-worked after a 1065 °C anneal. The as-received wire (specification AMS 5657) has a copper finish, which provides the proper lubrication for the heading process [4]. The *bright strand anneal condition* is also accepted, pas long as the mechanical properties and finish are within specifications. This condition requires no additional cold work of the wire [4].

The forming of the stems is a multistep process that primarily uses cold-working procedures to shape a rivet to dimension. The specific cold working processes that shape the stem are wiredrawing, stem heading, and threadrolling. Wiredrawing is the first step of forming the stem;

this process improves dimensional accuracy and surface finish. The result of this cold drawing process is that the resulting stem has developed different mechanical properties than the as-received condition, with diameter and shear ring tolerances within 0.0005 inches (per Cherry Aerospace specification) [5, 3]. Figure 3 shows a schematic of a typical die that the wire is pulled through to form the cold worked stem.

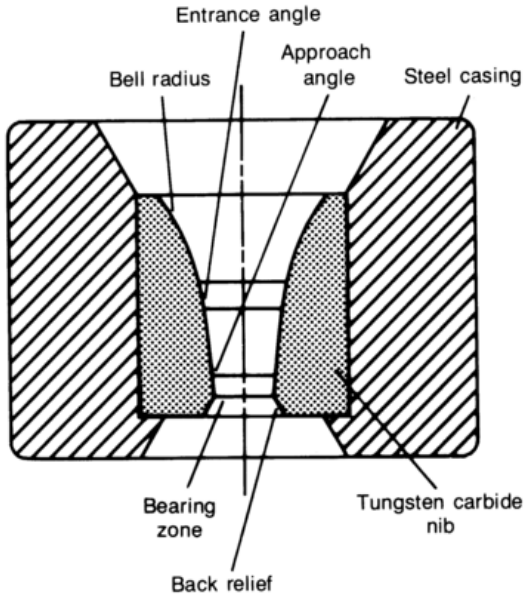

Figure 3. A wiredrawing die coldworks the wire by elongating the grains of the metal in order to reduce its cross-sectional area, so that it may proceed through the exit of the die. The result is a metal with a higher tensile strength and lower ductility. [5]

The second cold working step is stem heading: the process by which the newly dimensioned wire is shaped by severe, cold, plastic deformation. The stem is formed by moving through a series of six-dies of a progressive cold-heading machine that continually grips and ungrips the piece as it moves through the machine. Figure 4 is an example of a six-die cold heading machine. The hardness, strength, and microstructure are carefully controlled by heat treatment after the stem is formed. [6]

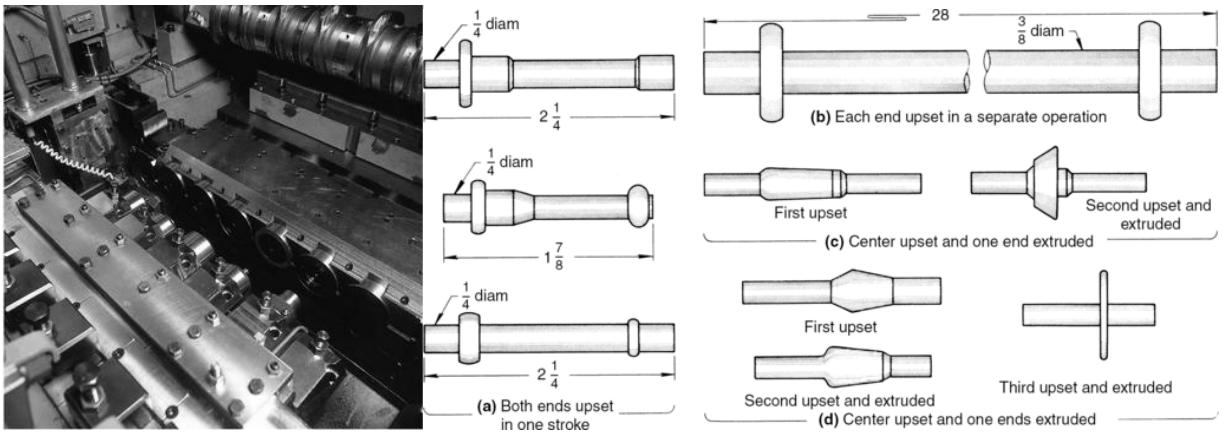

Figure 4. A six-die cold heading machine can make the various contours that are associated with rivet production. [7]

The last step of forming the stem of the rivet is thread rolling, a cold-forming process for producing threads by rolling the impression of hardened steel dies into the surface of a cylindrical bank. [8] In contrast to thread cutting and thread grinding, thread rolling does not remove metal from the work piece. Thread rolling displaces the surface metal to form roots and crests of a thread. Because of this deformation, the worked metal is appreciably stronger and harder than the original blank work piece. [8]

The emphasis of this investigation is not the forming process but the effects of the forming process on the microstructure of the stem of the CherryMAX® blind rivet. The shear ring (the circled portion in Figure 5), is the main concern. This portion is critical to the proper installation of the blind rivet. If it breaks too soon, the collar does not deform. If it breaks too late, or not at all, the stem will not break flush with the top of the rivet. Both scenarios cause improper installations and are a result of a shear strength above or below the optimum range. The current solution calls for adjusting the thickness of the shear ring to achieve shearing within the optimum range. This is a time consuming process. The ideal manufacturing process would exclude this adjustment and would change the strength through an adjustment of the current heat treatment process.

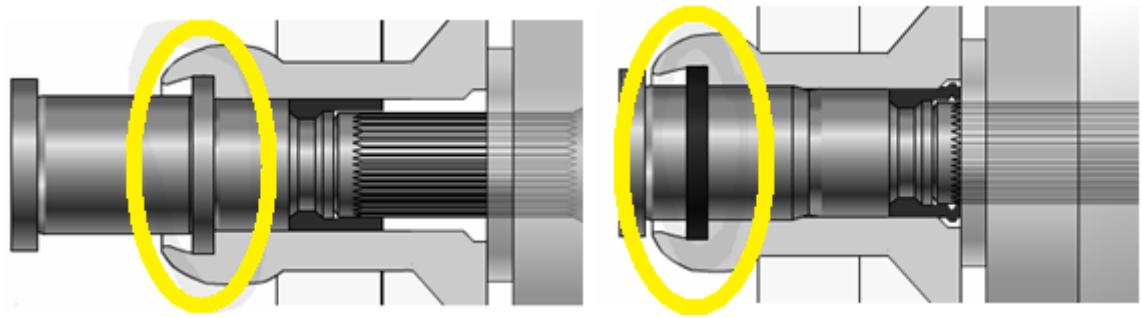

Figure 5. The ability of the shear ring (the circled portion) to shear within an optimum range of strengths is imperative to the proper function of the blind rivet. [3]

5.2.1 Semi-Austenitic Stainless Steels

The first discovery of a true stainless steel is accredited to Harry Brearley of Sheffield UK [9]. In 1913, Brearley added chromium to molten iron to produce an alloy with 12.8% chromium that resisted corrosion. The corrosion resistance occurs when the chromium reacts with oxygen in the atmosphere and forms a passive layer of chromium oxide on the surface of the alloy. By 1930, several types of stainless steel had been discovered, including precipitation hardenable stainless steel, discovered by William J. Kroll of Luxembourg. Kroll added titanium to the alloy, resulting in precipitation hardening capabilities [10].

Precipitation hardening (PH) stainless steels are iron-chromium-nickel alloys that undergo an increase in strength upon formation of precipitates that populate an austenitic or martensitic matrix. Precipitates form from one or more of the following elements: aluminum, copper, molybdenum, niobium, and titanium. The three categories of PH stainless steels are austenitic, martensitic, and semi-austenitic. The PH stainless steels are grouped into these categories depending on their martensite start and finish temperatures (M_s and M_f) and their crystal structure upon cooling from an elevated solution treatment temperature (Figure 6). [11]

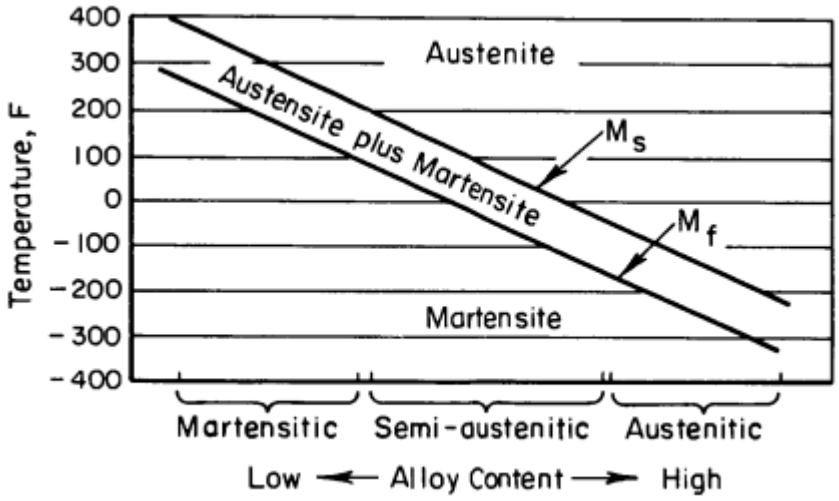

Figure 6. The effect of alloy content on the transformation temperature of stainless steels [11].

PH 15-7 Mo is a semi-austenitic alloy with its composition balanced to ensure a martensite start temperature well below room temperature (Figure 7). The precipitates that form in this specific alloy are β-NiAl and Ni_3Al [4]. Due to the substitution of 2% chromium with molybdenum, PH 15-7 Mo (UNS15700) is a higher strength variation of 17-7 PH, but requires identical heat

treatment procedures [4]. Many trends in responses to heat treatment of 17-7 can be correlated to similar trends in 15-7 Mo [11] [12].

COMPOSITION	(wt %)
Carbon	0.09 max.
Manganese	1.00 max.
Phosphorus	0.040 max.
Sulfur	0.040 max.
Silicon	1.00 max.
Chromium	14.00 – 16.00
Nickel	6.50 – 7.75
Molybdenum	2.00 – 3.00
Aluminum	0.75 – 1.50

Figure 7. Composition of PH 15-7 Mo when manufactured by AK Steel. [13]

In semi-austenitic stainless steels, cooling to room temperature yields a microstructure showing evidence of rather soft austenite not yet transformed to martensite. The current heat treatment process to promote martensite formation in PH 15-7 Mo involves an austenitizing treatment of either 760 °C (1400 °F), or 954 °C (1750 °F). At 760 °C, this step in the process precipitates chrome carbides along grain boundaries, resulting in the destabilization of austenite upon cooling from the austenitizing temperature [14]. The lower stabilizing temperature forms more particles at the grain boundaries due to the positive slope of the solvus line for both chromium and for carbon. This means that there is a higher solubility of chromium and carbon in austenite at 954 ° C, resulting in less driving force to precipitate carbides and therefore a more stable austenitic crystal structure upon cooling. A PH stainless steel that is austenitized at the higher temperature (954 °C) will have a higher strength, but require a refrigeration treatment to complete the transformation of austenite to martensite. In contrast, an alloy austenitized at 760 °C will completely transform to martensite upon cooling to room temperature (Figure 6) [11].

The next step is to age harden, or expose the alloy to an elevated temperature of around 510-565 °C. Diffusion rates of solute particles are negligible at lower temperatures, so precipitation does not occur naturally. The precipitation of submicroscopic intermetallic compounds occurs along crystallographic planes of the matrix material. Severe internal strain is introduced by the formation of precipitates because the lattice parameters of the particles differ from that of the matrix. The hardening effect of aging is due to the development of the strained condition that inhibits the motion of dislocations in the material. [11]

5.2.2 Heat Treatment and Precipitation Strengthening of PH 15-7 Mo Stainless Steel

The thermal treatments for the semi-austenitic stainless steel stems include solution heat treating, austenitizing, refrigeration, and precipitation hardening. Solutionizing and annealing eliminates the effects of the cold working and promote a uniform microstructure. Refrigeration allows for the transformation of austenite to martensite, and precipitation hardening gives the steel its desired strength and corrosion resistance. Table 1 is an overview of the two different options for heat treating PH 15-7 Mo Stainless steel.

TABLE 1 – STANDARD HEAT TREATMENTS

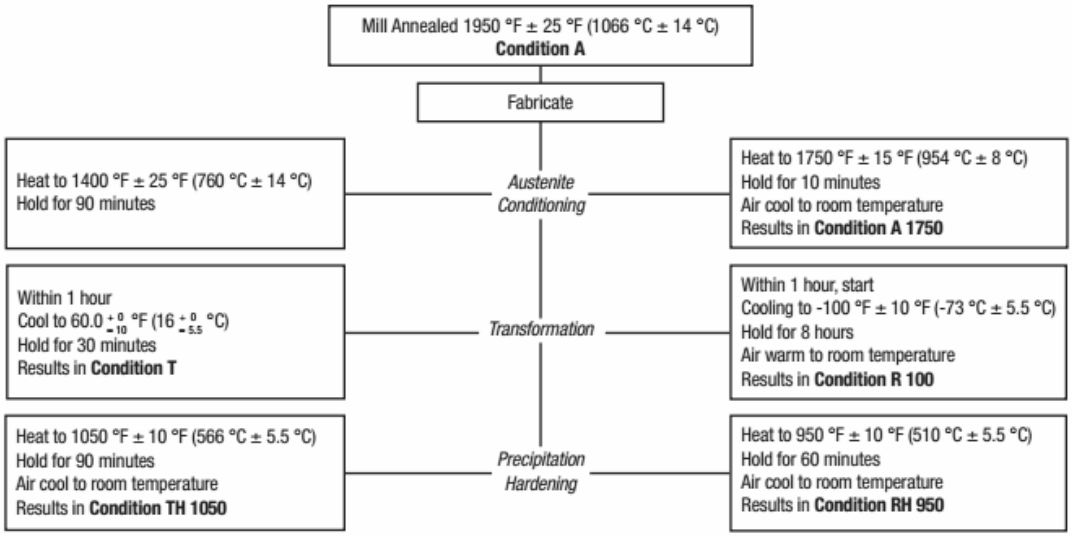

Note: Full TH 1050 properties may not be developed when PH 15-7 Mo Stainless Steel (cold worked) is heat treated to Condition TH 1050. However, full properties will be developed by using one of the following methods:

1) Re-anneal the fabricated part to Condition A and heat treat to Condition TH 1050.

2) Heat treat fabricated part to an RH 1050 Condition.

3) Use a modified TH 1050 heat treatment.

Full strength is developed when heat treating parts to Condition RH 950.

Source: AK Steel PH 15-7 Mo specification sheet [13]

Solution heat treating, or annealing, serves a variety of functions, principally to remove the formation of martensite that was caused by wire drawing, stem heading, and thread rolling. It is essential to remove this martensite because it is non-uniform, leading to a range of responses from subsequent heat treatments. Highly cold worked regions of the part will have higher internal strain energy, requiring less thermal energy to drive the precipitation reaction in that region. [11]

Another function of annealing is to create a condition that allows subsequent strengthening mechanisms to occur (martensitic transformation and precipitation hardening). A critical aspect to the solutionizing anneal is thermally treating within the correct temperature range. [11]

Deviation from recommended annealing temperatures can result in poor mechanical properties. With higher than normal annealing temperatures, less martensite will form upon cooling and lower strength in the fully hardened condition will result. At lower than normal annealing temperatures, ductility is decreased after precipitation hardening. Table 2 shows the different mechanical properties achieved among the varying parameters for heat treatments.

TABLE 2 – TYPICAL ROOM TEMPERATURE MECHANICAL PROPERTIES*

Property	Condition							
	A	T	TH 1050	A 1750	R 100	RH 950	C	CH 900
UTS, ksi. (MPa)	130 (896)	145 (1000)	220 (1517)	150 (1034)	180 (1241)	245 (1689)	220 (1517)	265 (1828)
0.2% YS, ksi. (MPa)	55 (372)	90 (620)	205 (1413)	55 (372)	125 (862)	215 (1482)	190 (1310)	260 (1793)
Elongation, % in 2" (50.8 mm)	33	7	6	12	7	6	5	2
Rockwell Hardness	B88	C28	C45	B85	C40	C49	C45	C50

TABLE 3 – PROPERTIES ACCEPTABLE FOR MATERIAL SPECIFICATION

Property	Condition				
	A	TH 1050	H 925	C	CH 900
UTS, ksi. (MPa)	150 max (1034)	190 min. (1310)	225 min. (1552)	200 min. (1379)	240 min. (1655)
0.2% YS, ksi. (MPa)	65 max. (448)	170 min. (1172)	200 min. (1379)	175 min. (1207)	230 min. (1586)
Elongation, % in 2" (50.8 mm)	25 min.	–	–	1 min.	1 min.
0.20 – 0.1875 in. (0.51 – 4.76 mm)	–	5 min.	4 min.	–	–
0.10 – 0.0199 in. (0.25 – 0.50 mm)	–	4 min.	3 min.	–	–
Rockwell Hardness*	B100 max.	C40 min.	C46 min.	C41 min.	C46 min.

**Applies to material 0.010 in. (0.25 mm) and thicker. Selection of hardness scale is determined by material condition and thickness. Where necessary,superficial hardness readings are converted to Rockwell B or C.*

Source: [13]

Austenite conditioning and refrigeration cause the transformation of austenite to martensite. The martensite start and martensite finish temperatures are depressed with decreasing amounts of both chromium and carbon dissolved in austenite. Table 1 shows the two conditioning treatments that are used for PH 15-7 Mo stainless steel. At 954 °C, austenite has a higher solubility of chromium and carbon, which results in fewer chromium carbides ($Cr_{23}C_6$) that precipitate along grain boundaries and requires refrigeration to completely transform the austenite to martensite. The lower conditioning temperature of 760 °C results in a high presence of chromium carbides, only requiring lowering to room temperature for martensite to completely form. [11]

CherryMAX® rivet stems are austenitized at 954 °C in order to more effectively relieve residual stresses and produce uniform mechanical properties throughout the entire stem. The proprietary heat treatment is outlined by the right hand side of Table 1, but some changes are made in order to increase the corrosion properties of the stems. The use of a higher austenitizing temperature yields a stronger part when properly refrigerated to -73.33 °C for 8-9 hours. The higher strength is likely due to the formation of a martensite with a greater carbon content. [11]

For precipitation hardening of 15-7 Mo PH stainless steels, NASA suggests aging a precipitation hardening range between 454-565 °C (850-1050 °F), depending on the engineering application. Precipitation hardening of the semi-austenitic stems of the blind rivet occurs between 538 °C and 563 °C (1000-1045 °F), which according to Figure 8, is an overaging treatment. The aging treatment causes β-NiAl and Ni_3Al intermetallic compounds to precipitate out. Overaging improves toughness, ductility, and corrosion resistance, but at the cost of strength. [2] The aging temperature that produces the highest strength is 510 °C (Figure 8).

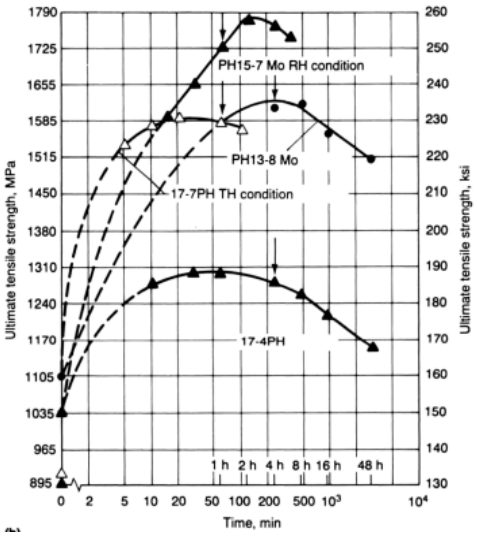

Figure 8. Aging curves at 510 °C for various semi-austenitic alloys. PH 15-7 Mo refrigeration hardened at -73.33 °C is the strongest semi-austenitic alloy shown [14].

5.2.3 Precipitation Formation and Ostwald Ripening

Age hardening is a thermally activated process, wherein diffusion increases to an appreciable level at temperatures where the supersaturated solid solution begins to nucleate solute-rich particles. This occurs because the solute is trapped in the solvent matrix. The concentration of solute is greater than the host matrix can dissolve in equilibrium conditions. [15] Thermodynamics states that the necessary conditions for particle precipitation are present, but the kinetics side of the situation states that the sufficient conditions for nucleation are not met at relatively low temperatures. At elevated aging temperatures, the activation energy required to

diffuse large amounts of solute is supplied by the thermal energy of the system. The presence of a supersaturated solution and sufficient activation energy satisfies both the thermodynamic and the kinetic requirements, resulting in the nucleation of solute-rich precipitates in the host matrix. [15]

In the PH 15-7 Mo alloy system, the 6.5-7.75 Wt. % Ni and 0.75-1.5 Wt. % Al are the solutes in the martensitic matrix. As in most age hardenable materials, the aging temperature affects the size of the precipitates. The higher the temperature, the greater the diffusion will be in the alloy and the larger the precipitate particles will be. This is because solute particles diffuse from areas of supersaturation to regions around precipitates. The concentration of solute around a small particle is greater than that around a larger particle, which leads to the net diffusion of solute in the direction of large precipitates. [15]

The growth of large particles in favor of small particles is called Ostwald Ripening. This occurs because the solute atoms diffuse from regions around small particles to regions around large particles. Ostwald Ripening can be modelled by the Cahn-Hilliard Equation. (Eq. 1) [16]

$$\frac{\partial c}{\partial t} = D\nabla^2\left(c^3 - c - \gamma\nabla^2 c\right) \qquad \text{Eq. 1}$$

Where:

= Change in concentration per unit time

D= diffusion coefficient (length^2/unit time)

∇^2= Laplacian or Gradient

$\mu = c^3 - c - \gamma\nabla^2 c$ = chemical potential (partial molar free energy)

The main result of Ostwald Ripening is the growth of ß-NiAl and Ni_3Al intermetallics that impede the movement of dislocations in the steel. This impedance to dislocation movement is the primary strengthening mechanism in precipitation hardening materials. The average radius is modelled by a mathematical equation for the average size of precipitates with respect to time. (Eq. 2) [17]

$$\langle R\rangle^3 - \langle R\rangle_0^3 = \frac{8\gamma c_\infty v^2 D}{9R_g T}t \qquad \text{Eq. 2}$$

Where:

$\langle R\rangle$= average radius of all the particles

γ = particle surface tension or surface energy

c_∞= solubility of the particle material

v = molar volume of the particle material

D = diffusion coefficient of the particle material
R_g = ideal gas constant
T = absolute temperature and
t = Time

This model was determined by Lifshitz and Slyozov in 1958. Over time, the average precipitate size increases. With greater diffusivities, the rate of precipitate formation (hardening) increases. Atoms in crystalline orientation are less energetic than those in solution surrounding the particles. The free energy can be decreased by forming a larger precipitate via the diffusion of solute atoms to the precipitate surface. This decrease in free energy is the driving force for precipitate growth once solute atoms have diffused to the particle. [17]

5.2.3a Ostwald Ripening in Detail

The growth of the average precipitate size over time is known as Ostwald Ripening and occurs because the material is at a lower energy state when super saturated solute atoms become fully segregated to areas of precipitate formation by the mechanism of diffusion. These precipitates grow after nucleation and further segregate the solute atoms. The uphill diffusion that occurs along with the growth of precipitates is caused by the decrease in total free energy of the system as a whole. The negative change in free energy means the reaction is spontaneous when given the proper activation energy and the diffusion of the solute is appreciable. This activation energy is provided by the thermal energy of the material system. [15] The thermal energy and rate of diffusion increase with temperature, which is why the process of precipitation hardening occurs at elevated temperatures. These temperatures can be as low as 300°C. The growth rate of particles is often modeled by the incremental change in volume over an incremental change in time, which increases with increasing temperature (Eq. 2). It is experimentally observed that the large solute-rich precipitates grow in preference to, and at the expense of smaller precipitates because the surface energy to volume ratio of a larger particle is less than that of a small particle. The surface energy of a system is minimized with a small number of large precipitates, as opposed to a large number of tiny precipitates. [15]

5.2.4 Property Dependence on Precipitation Hardening Heat Treatment Parameters

The parameters of each step in the heat treatment of PH 15-7 Mo affect the final properties of the alloy (Figure 9). The solution treatment temperature for the CherryMAX® rivet stems is 1052 °C (1925 °F) for 90 minutes. With an increase in the temperature for this process, one would expect to have a final strength less than the strength from the current treatment.

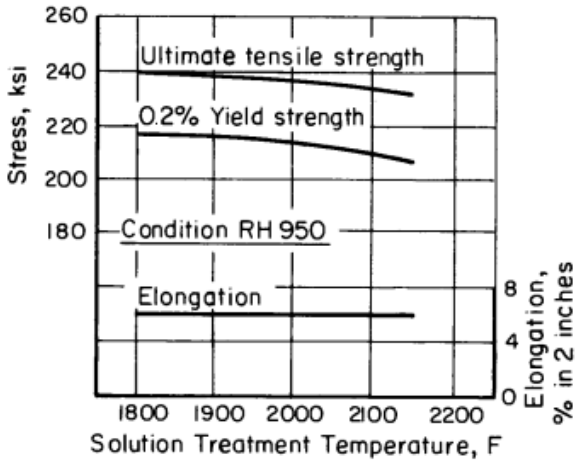

Figure 9. Effect of solution heat treatment temperature on the properties of PH 15-7 Mo in the RH 950 condition [11].

The current austenitizing treatment for the PH 15-7 Mo rivet stems is 954 °C (1750 °F) for 105 minutes. Increasing the temperature for this treatment would produce a sharp decline in strength, while a decrease in the temperature would produce a small increase in strength (Figure 10).

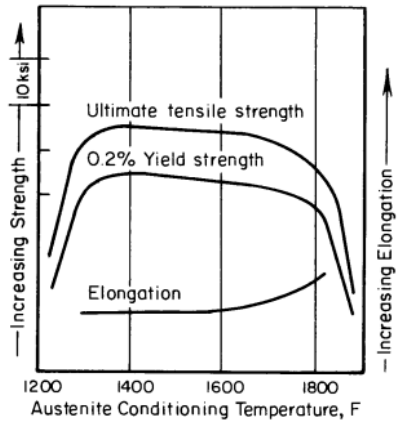

Figure 10. Effect of austenite-conditioning temperature on the mechanical properties of PH 15-7 Mo in the RH 950 condition. [11]

The refrigeration treatment causes austenite to transform into martensite. To achieve the highest strength, is it recommended to refrigerate PH 15-7 Mo for at least eight hours [8]. Cherry Aerospace refrigerates their rivet stems for eight hours and fifteen minutes at -77.33 °C.

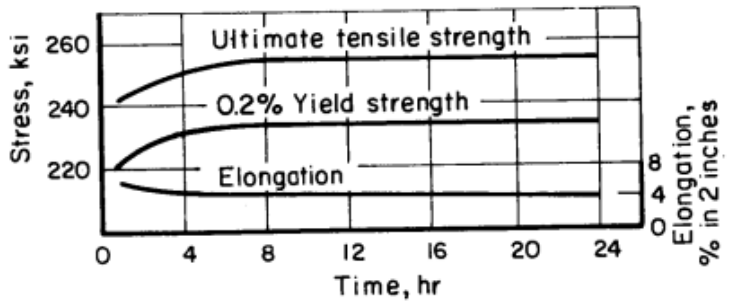

Figure 11. Effect of variation in the refrigeration time at -77.33 °C on the mechanical properties of PH 15-7 Mo, condition RH 950

Cherry Aerospace age hardens the PH 15-7 Mo rivets stems in a vacuum furnace at a range of temperature from 543 to 557 °C (1010-1035 °F), depending on the section thickness of the product. This treatment results in an overaged condition, characterized by a strength less than maximum, but a greater resistance to corrosion [2, 18]. PH 17-7, almost identical to PH 15-7 Mo, peaks in strength approximately at 482 °C. (900 °F) [11]

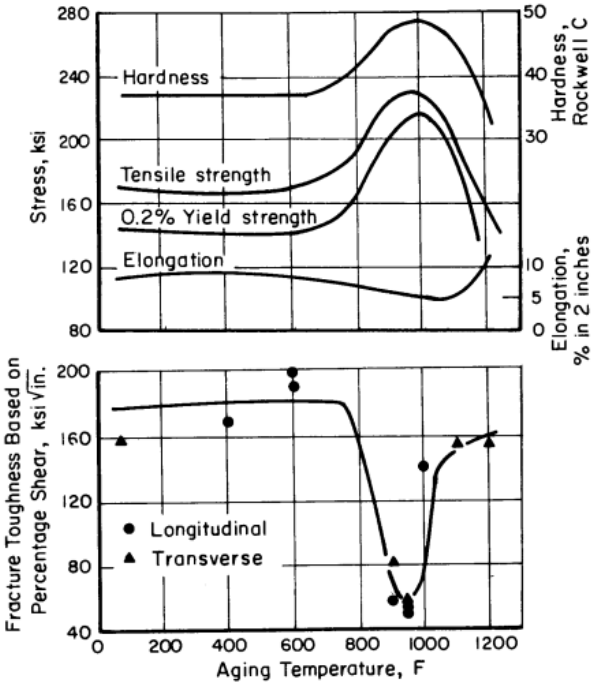

Figure 12. Effect of Aging temperature on the mechanical properties of PH 15-7 Mo in the RH condition.

The strength of the 17-7 PH rises rapidly after aging for as little as five minutes. After 30 minutes at the aging temperature, the strength begins to slightly decrease as Ostwald ripening occurs. Cherry Aerospace ages the PH 15-7 Mo rivet stems for four hours, much longer than thermodynamically necessary.

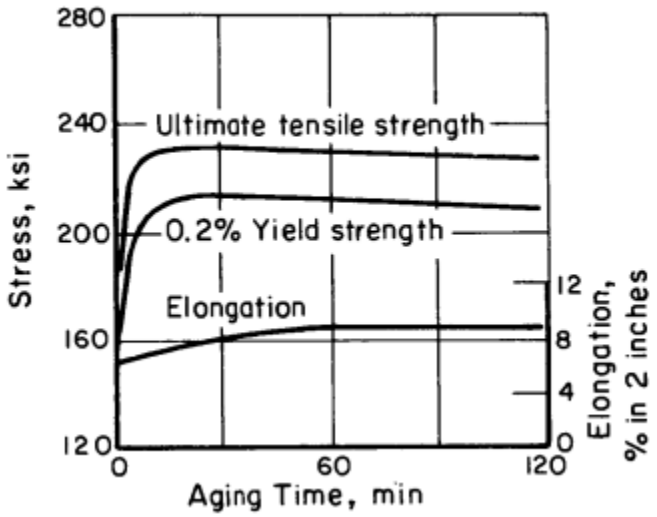

Figure 13. Change in tensile properties of 17-7 PH in the RH condition with increasing time at the aging temperature.

6. Experimental Procedure

6.1 Mechanical Testing

Samples were pulled from 6 different manufacturing operations and tested using 4 of those steps in the manufacturing process. The maximum shear strength of the rivet stems was evaluated using a double shear compression test, according to the National Aerospace Standards Metric (NASM) 1312-13A.

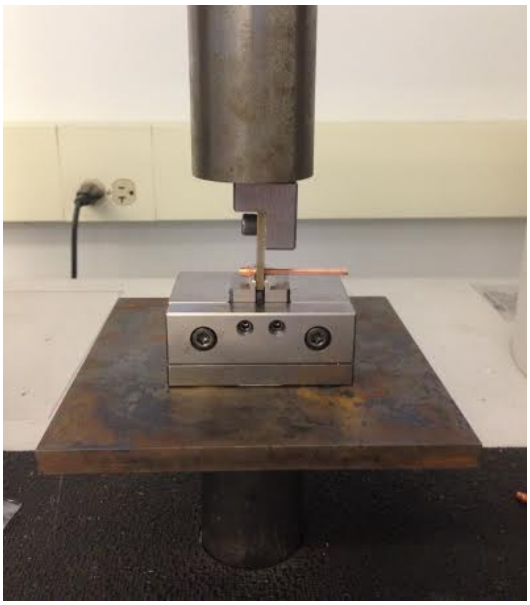

Figure 14: The test fixture rests on a hardened steel plate and consists of a lower component that supports the rivet stem and an upper component that applies the load.

Using experimental stiffness values, a standard-specified load rate was converted to extension rate as required by NASM 1312-13A. For example, the load rate for a nominal diameter of 0.125 inches is 2,480 lb/min. Using the slope from the elastic region of the load of curve of 66,667 lb/in, an extension rate of 0.0372 in/min was calculated. (Equation 1)

$$\mathbf{[Slope\ (lb/in)]^{-1} \times Load\ Rate\ (lb/min) = Extension\ Rate\ (in/min)} \quad \text{(Eqn. 1)}$$

After measuring the diameter of the grip section, samples were loaded into the double shear compression test fixture. As a compressive load was applied, the Bluehill testing software recorded the maximum load and plotted a load curve for each sample until failure. (Appendix) From each operation and each different lot, 5 to 15 samples were tested and recorded on a single load curve. One-way analysis of variance (ANOVA) provided the averages of each test group and the variance within the operations. The square-root of the value for variance provided the standard deviation within each data set.

6.2 Aging Treatments

The aging treatments were performed by dividing the lots into separate aluminum foil baskets. The samples were laid flat and were aligned the same way. The furnace door was opened briefly to insert baskets one at a time. Aging time began once the furnace returned to its original temperature, which was approximately 2 minutes. The aging treatments ranged in temperatures from 950 °F to 1040 °F, increasing in 18 °F increments. Different samples from each operation and lot were aged for 1.5 hours at 950 °F (to simulate peak aging), 968 °F , 986 °F , 1004 °F , 1022 °F, and 1040 °F for 4 hours (to simulate a range of overaged conditions). After aging, the samples were pulled from the furnace, air-cooled at room temperature, and placed in the appropriate organizing bin to keep track of the samples.

7. Results

The goal of this project was to establish a correlation between incoming material strength and final shear strength. Referencing Figure 15, there was no distinct correlation between these two properties. OP 32 is representative of the as-received condition, while rivet stems labeled as OP 127 are tested post-aging.

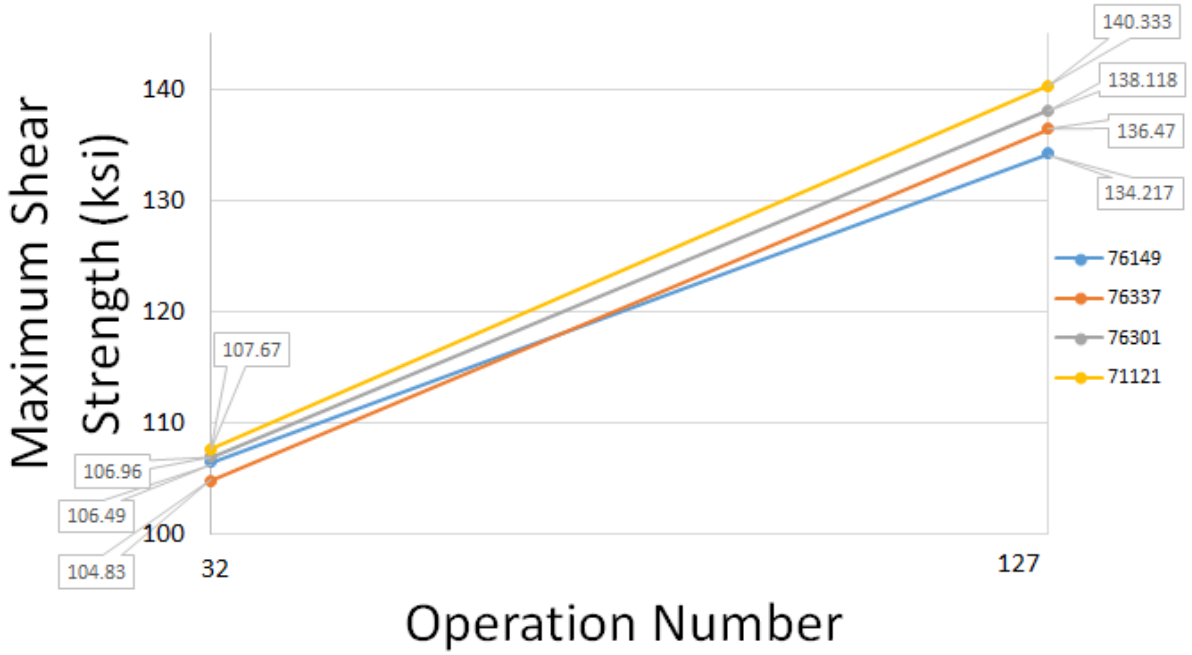

Figure 15: There is a marked increase in strength from OP 32 to OP 127, with lot 76149 being the outlier.

In order to have a better understanding of the lack of correlation, additional testing was performed to track shear strength throughout the entire manufacturing process (Figure 16). From OP 32 to OP 71, the response to the anneal was a decrease in strength just as often as it was an increase. Next, there was a general decrease in strength from OP 71 to OP 123, indicating the formation of chrome carbides ($Cr_{23}C_6$). However, material from A-cert 76149 does not follow this trend.

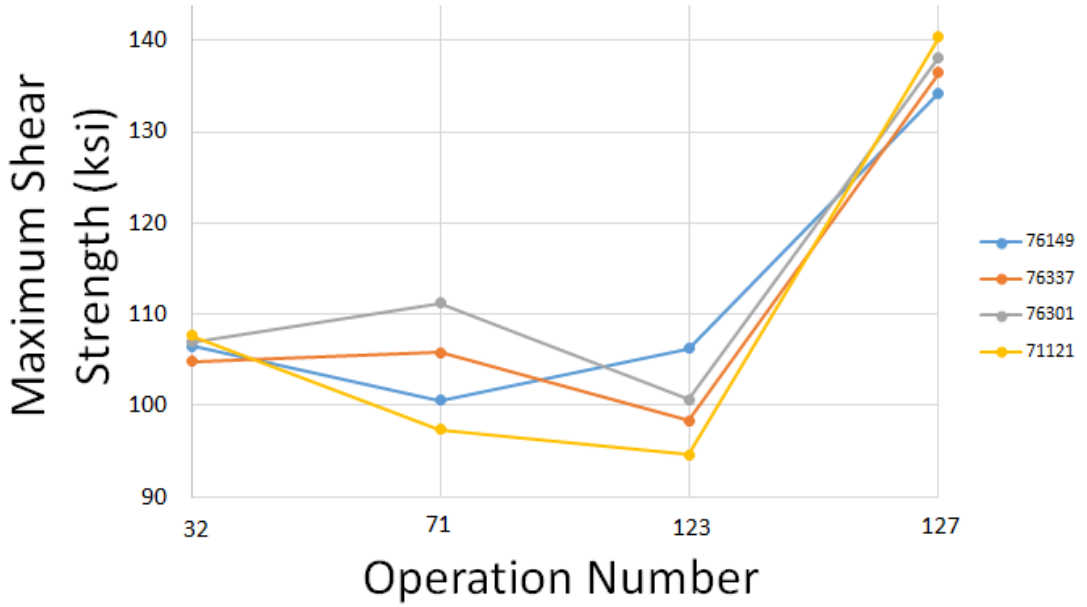

Figure 16: No definitive trends exist between operations throughout the manufacturing process. The strongest incoming material was not necessarily the strongest material throughout the manufacturing process.

There was a definitive increase in strength from OP 32 to OP 127. Even with this general increase in strength, no correlation could be made between the incoming shear strength and the final shear strength. Material from A-cert 71121 was the strongest at OP 32 and at OP 127. However, material from A-cert 76337 was the weakest at OP 32, but was NOT the weakest at OP 127. With only four lots to compare, there was not enough evidence to propose any correlation.

In the graph of maximum shear strength vs. temperature (Figure 17), the general trend was decreasing strength with increasing temperature. However, certain lots exhibit uncharacteristic responses to the experimental aging treatments. For example, material from A-cert 71121 peaks in strength near 986°F (530°C). This shift in peak strength could be due to a compositional difference that inhibits formation of precipitates until higher aging temperatures. The kinetics of this process was outside the scope of this project, but could be studied with future microstructural analysis.

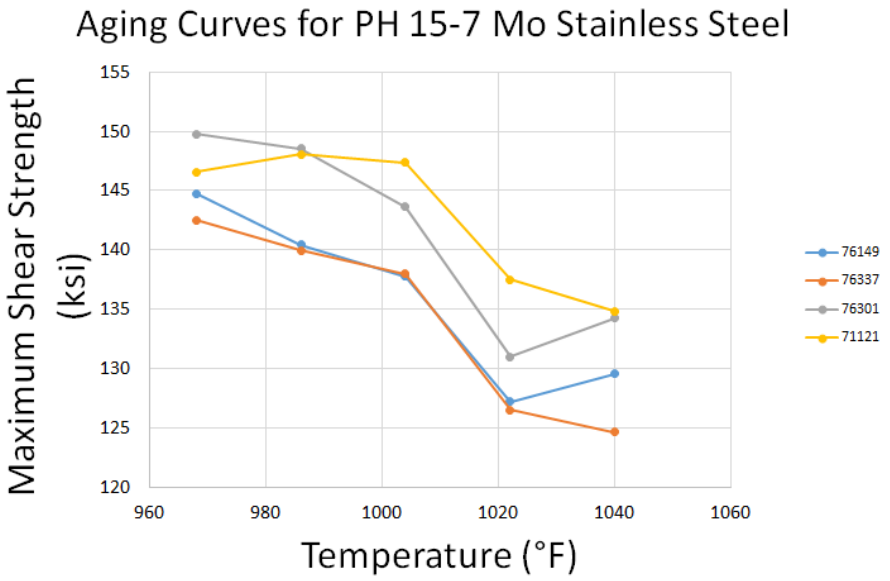

Figure 17: The maximum shear strength vs. temperature plot represents the aging curve. Cherry Aerospace slightly overages rivet stems as to improve corrosion properties.

The composition of the rivet stems did not vary appreciably among lots (Table 4). The most notable difference was the weight percent of aluminum in lot 71121. It has 10.44% higher aluminum content at 1.31 wt% aluminum, whereas the other lots have 1.18 wt% Al. Aluminum content is important because it is the limiting reagent for the precipitation of β-NiAl and Ni_3Al precipitates.

Chromium and nickel equivalents were used in an effort to correlate how each material would responded to the same heat treatments (Table 4). It was reported that all the A-cert numbers have

nearly identical chromium and nickel equivalents and therefore would respond nearly identical to the same heat treatments. The greatest difference was between A-Cert numbers 76149/76337 and A-Cert 71121. A-Cert number 71121 had a 1.75% lower chromium equivalent than the other lots. However, 71121 also had the highest weight percent aluminum

Table 3: The Chemical Compositions and Cr/Ni Equivalents for Each Lot (Weight %)

WOID	A-Cert	%C	%Mn	% Si	%P	%S	%Cr	%Ni	%Al	%Mo	%N	Cr Equivalent	Ni Equivalent
88030569	76149	0.08	0.56	0.34	0.014	0.001	15.3	7.13	1.18	2.14	0.016	9.81	17.95
88040122	76337	0.08	0.56	0.34	0.014	0.001	15.3	7.13	1.18	2.14	0.016	9.81	17.95
88046783	76301	0.07	0.58	0.28	0.014	0.001	15.37	7.27	1.18	2.18	0.024	9.66	17.97
88047697	71121	0.07	0.54	0.25	0.015	0.001	15.43	7.27	1.31	2.15	0.024	9.64	17.955

It should be noted that the rivet stems aged in the Materials Engineering Department furnaces had an average of 6.75 ksi lower shear strength values than those heat treated in the Cherry Aerospace furnaces (Figure 18).

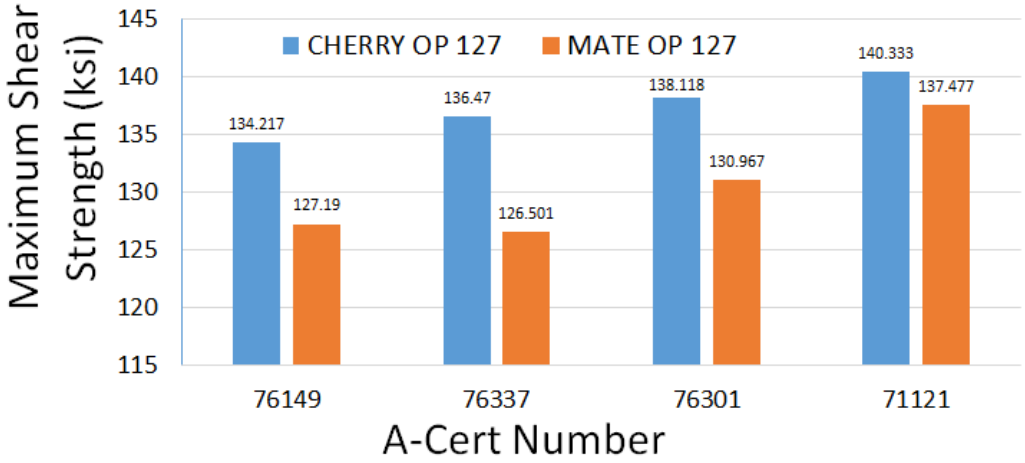

Figure 18: Aging treatments in the MATE Cal Poly furnaces produced lower shear strength values possibly due to lag and ramping times, part volume, and other factors.

8. Discussion and Further Research

This research and mechanical testing ultimately provides Cherry Aerospace with a baseline for the shear strength of the rivet stems. However, looking at Figure 15 we can see that from operations 32 to 127, there were no definitive trends for the lots because the trend lines intersect each other throughout the different operations. The strength was unpredictable among lots from operation to operation. Even though we cannot draw significant conclusions from this data, Cherry Aerospace now has a baseline for future work. Additionally, the lack of a definitive

correlation between incoming shear strength and final shear strength means that the aging curves are unable to be utilized to recommend adjustments to the current aging treatment (Figure 17).

The mid-process anneal after OP 32 can both increase or decrease strength. Two lots increased in strength while two others decreased. The increase in strength could be due to a refinement of the grain size, while a decrease in strength could be explained by the relieving of residual stresses from prior cold working. Metallographic imaging would be useful in future work to analyze what is happening to the stainless steel wire from OP 32 to OP 71.

There was a general decrease in strength from OP 71 to OP 123, indicating the formation of chrome carbides ($Cr_{23}C_6$). As the alloying elements of chromium and carbon atoms were concentrated along the grain boundaries, the overall strength was predicted to decrease. The one exception is that material from A-cert 76149 does not follow this trend, and further work should be conducted to examine the microstructure and determine the cause of the outlying result.

When examining the response to heat treatment of two lots of identical composition (76337 and 76149), their shear strength values are not identical, nor do they follow any similar trends in strength. This could indicate that there are variables in the manufacturing processes that are affecting the final shear strength of the rivet stems. It is recommended that any continuation of this research investigate the response of a single lot to identical heat treatments, but over the course of a year. This would determine if the variations in the processing of the rivet stems affects final shear strength as opposed to compositional or as-received strength variations.

While on the topic of composition, if the relative amounts of aluminum and nickel vary across A-cert numbers, the amount and size of β-NiAl and Ni_3Al precipitates would also be expected to vary. This theory could be tested by quantifying the average size and density of precipitates using X-Ray Diffraction (XRD) and possibly a scanning electron microscope (SEM). Cherry Aerospace precipitation hardens the rivet stems near 552 °C (1025 °F) for 4.25 hours, which was an aging treatment at a higher temperature and for a longer time than the recommended peak aged condition: 510 °C (950 °F) for 1 hour. Precipitate size is a function of both temperature and time. In lots with a higher weight percent aluminum (say 1.50 wt %), there may be a higher number of small precipitates after heat treatment. In lots with a lower weight percent aluminum (say 0.75 wt%), there may be a fewer, larger precipitates after heat treatment. [17]

It should be noted that the shear strength was significantly different from furnace to furnace, even with similar aging temperatures. This was to be expected due to the size of the furnaces and the number of parts ran at one time. Cherry Aerospace uses large industrial grade furnaces, while the Materials Engineering Department uses smaller, experimental furnaces. For Cherry Aerospace furnaces, the time for both the furnace and the parts to reach temperature after opening the furnace could be greater compared to the relatively short amount of time it takes for the department furnaces to rise to full temperature. Cherry Aerospace also processes around

50,000 parts at a time, whereas the experimental heat treatments in this procedure treated only 10-30 parts at one time. The combination of these two factors results in the MatE furnaces producing over-aged parts when compared to Cherry Aerospace heat treated parts.

It is also possible that the variations seen at the end of the manufacturing process stem from the processing of the wire at the mill. Occasionally, the mill cold works the PH 15-7 Mo to achieve Cherry's requirement of 105-125 ksi yield strength. The extent to which the wire has to be cold worked may be dependent on compositional differences, which can in turn affect the properties after heat treatment. The microstructure of the stainless steel ultimately dictates the mechanical properties, and the microstructure may reveal the root cause of Cherry Aerospace's concern about product variance.

It is noted in the load curves (Appendix) that there was an observable variance in ductility within lots at the same operation. A drawback of the double shear compression test was that ductility can be difficult to accurately measure. Testing for impact toughness would take into account both strength and ductility. It is recommended that future work utilize the Charpy Impact Test to simulate the high strain-rate conditions present in rivet installation. This may lead to data that correlates to other material properties or composition.

Also, for future work, it would be helpful to know which lots pass and which ones fail because the lots that fail could reveal other factors that may influence an AQL failure. Furthermore, it would be helpful if the record keeping of the reworked parts was in digital form so that the data would be easily accessible for study. It is additionally recommended that there is a refinement of the Pass/Fail procedures to better ensure lots need to be reworked. Right now, the criterion for a "pass" is 2 out of 20 tests are allowed to fail, whereas a "fail" is constituted by 3 or more out of 20 failing. The difference between two and three failures is not significant and could be refined. it is recommended to test an additional 20 samples upon a "Fail" to ensure that the lot needs to be reworked.

9. References

1. *Dictionary of Metals*. Reference Information Library, added to *ASM Handbooks Online: Desk Editions and General References,* ASM International, 2013.
2. Campbell, F. C. Manufacturing Technology for Aerospace Structural Materials. Amsterdam: Elsevier, 2006. Print.
3. Cherry Aerospace. "Process Manual." CHERRYMAX ® Process Manual (n.d.): n. pag.www.cherryaerospace.com. Web. 25 Nov. 2014.
4. Davis, J. R. *Stainless Steels Specialty Handbook*. N.p.: ASM, n.d. *Google Books*. Web. 25 Nov. 2014.
5. A.B. Dove, Steel Wire, *Properties and Selection: Irons, Steels, and High-Performance Alloys*, Vol 1, *ASM Handbook*, ASM International, 1990, p 277–288.
6. Cold-Finished Steel Bars, *Properties and Selection: Irons, Steels, and High-Performance Alloys*, Vol 1, *ASM Handbook*, ASM International, 1990, p 248–271.
7. Source: T. Padfield, Cold Heading, *Metalworking: Bulk Forming*, Vol 14A, *ASM Handbook*, ASM International, 2005, p 383–404.
8. Thread Rolling, *Metalworking: Bulk Forming*, Vol 14A, *ASM Handbook*, ASM International, 2005, p 489–504.
9. Thomas, G.P. "The History of Stainless Steel – Celebrating 100 Years." *The History of Stainless Steel – Celebrating 100 Years*. A to Z of Materials, 11 Mar. 2013. Web. 30 Nov. 2014.
10. Gray, Jane. "100 Years of Stainless Steel." The Manufacturer. N.p., 6 Feb. 2013. Web. 30 Nov. 2014.
11. Slunder, C. J., A. F. Hoenie, and A. M. Hall. "Thermal and Mechanical Treatments for Precipitation-Hardenable Stainless Steels and Their Effect On Mechanical Properties." *NASA Technical Memorandum* 53578th ser. TM.X (1967): 8-204. Web. 25 Nov. 2014.
12. J. Douthett, Heat Treating of Stainless Steels, *Heat Treating*, Vol 4, *ASM Handbook*, ASM International, 1991, p 769–792. (was 6)
13. "PH 15-7 Mo Stainless Steel." Ak Steel. AK Steel, n.d. Web. <http://www.aksteel.com/pdf/markets_products/stainless/precipitation/15-7_mo_data_bulletin.pdf>.
14. Davis, J. R. Alloy Digest Sourcebook: Stainless Steels. Materials Park, OH: ASM International, 2000. Print.
15. Callister, William D. Fundamentals of Materials Science and Engineering: An Integrated Approach. Hoboken, NJ: John Wiley & Sons, 2005. Print.
16. Wikipedia contributors. "Cahn–Hilliard equation." *Wikipedia, The Free Encyclopedia*. Wikipedia, The Free Encyclopedia, 20 Apr. 2013. Web. 5 Dec. 2014.
17. Lifshitz, I.m., and V.v. Slyozov. "The Kinetics of Precipitation from Supersaturated Solid Solutions."Journal of Physics and Chemistry of Solids 19.1-2 (1961): 35-50. Web.
18. Lippold, John C., and Damian J. Kotecki. *Welding Metallurgy and Weldability of Stainless Steels*. Hoboken, NJ: John Wiley, 2005. Print.

10. Appendix

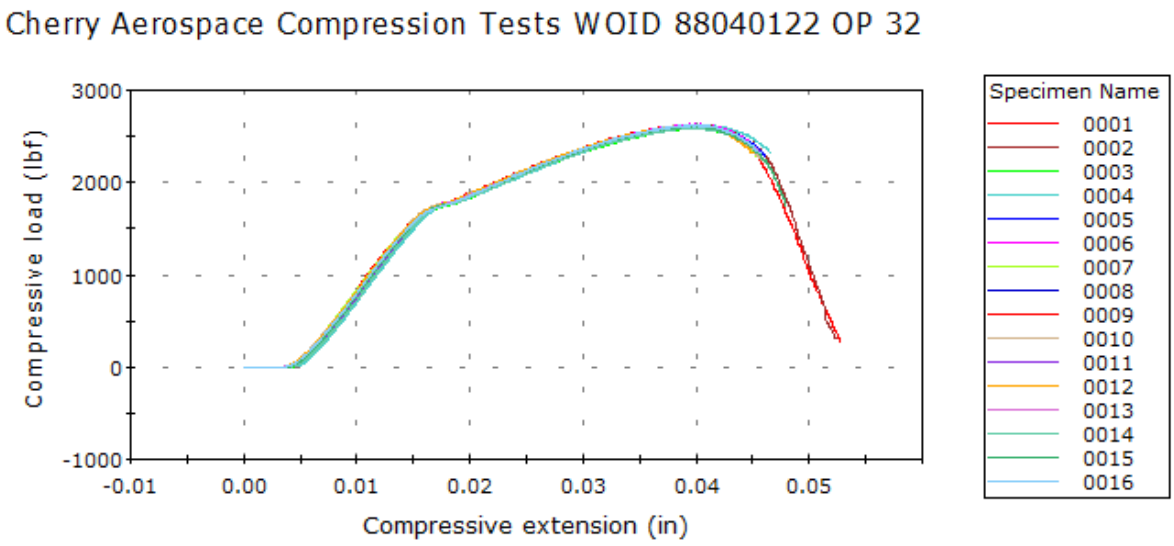

OP 32	Specimen label	Maximum Load (lbf)	Extension at Maximum Comp. load (in)
1	0001	2627.05	-0.0394
2	0002	2632.53	-0.0403
3	0003	2590.38	-0.0403
4	0004	2620.88	-0.0403
5	0005	2622.57	-0.0399
6	0006	2633.97	-0.0399
7	0007	2619.07	-0.0394

8	0008	2617.02	-0.0399
9	0009	2620.64	-0.0399
10	0010	2620.57	-0.0394
11	0011	2617.18	-0.0399
12	0012	2618.32	-0.0394
13	0013	2620.23	-0.0399
14	0014	2594.86	-0.0399
15	0015	2612.60	-0.0399
16	0016	2626.02	-0.0399

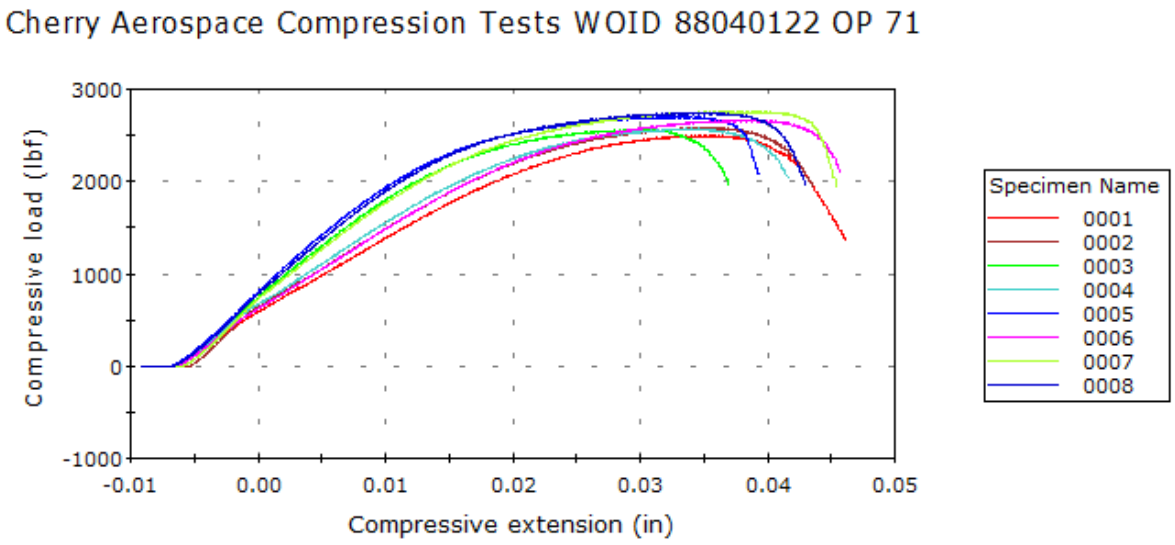

71	Specimen label	Maximum Load (lbf)	Extension at Maximum Comp. load (in)
1	0001	2501.88	-0.0355
2	0002	2586.70	-0.0355
3	0003	2562.35	-0.0303
4	0004	2574.52	-0.0341
5	0005	2703.04	-0.0336
6	0006	2668.23	-0.0383
7	0007	2761.88	-0.0378
8	0008	2747.30	-0.0346

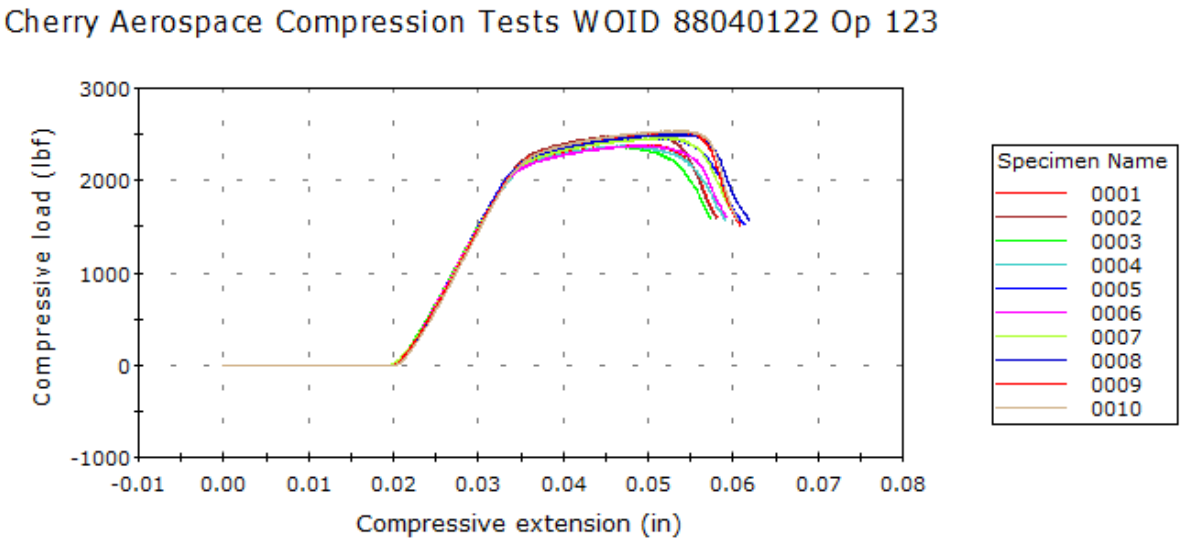

123	Specimen label	Maximum Load (lbf)	Extension at Maximum Comp. load (in)
1	0001	2386.40	-0.0496
2	0002	2506.69	-0.0496
3	0003	2368.17	-0.0468
4	0004	2379.35	-0.0478
5	0005	2464.98	-0.0520
6	0006	2382.47	-0.0492
7	0007	2467.54	-0.0520
8	0008	2503.98	-0.0534
9	0009	2534.15	-0.0529
10	0010	2540.17	-0.0529

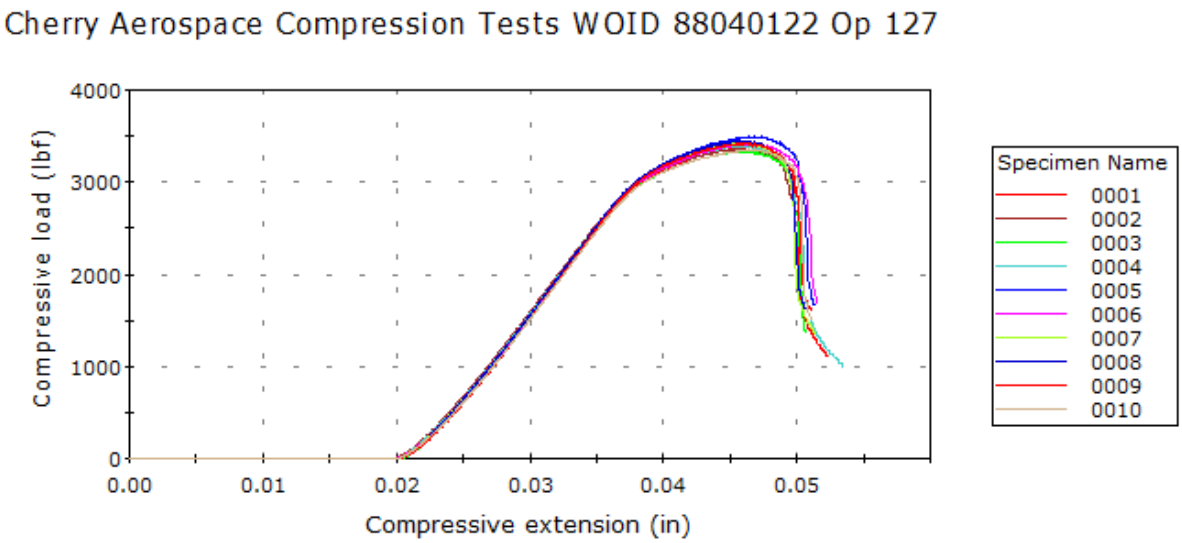

127	Specimen label	Maximum Load (lbf)	Extension at Maximum Comp. load (in)
1	0001	3387.08	-0.0464
2	0002	3362.49	-0.0454
3	0003	3336.43	-0.0459
4	0004	3391.53	-0.0459
5	0005	3495.74	-0.0468
6	0006	3418.61	-0.0464
7	0007	3435.97	-0.0459
8	0008	3451.02	-0.0459

9	0009	3424.39	-0.0459
10	0010	3356.32	-0.0468

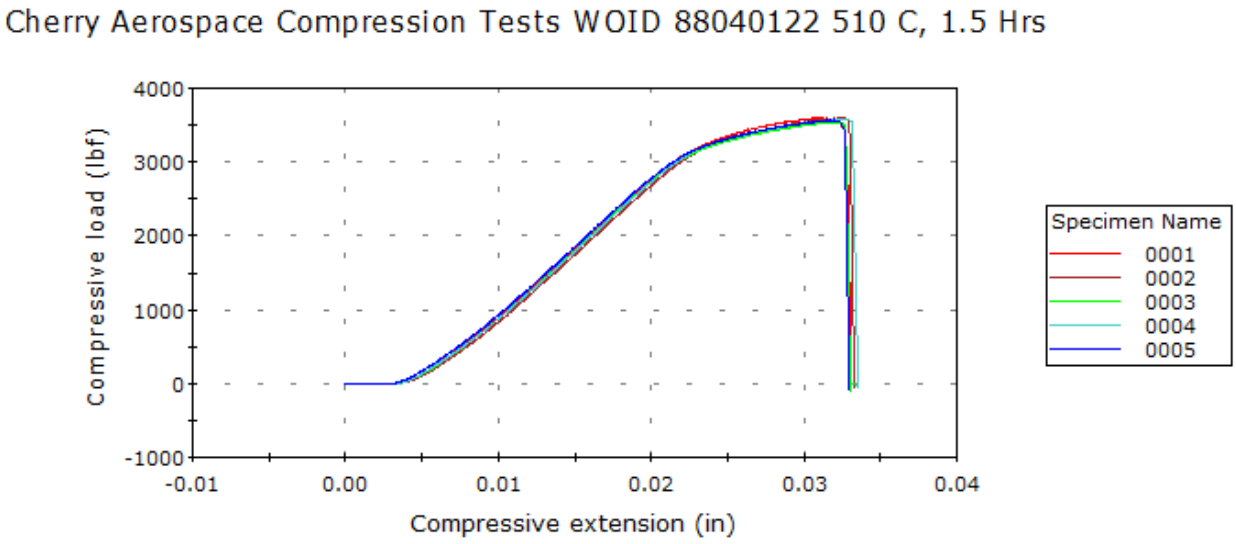

510	Specimen label	Maximum Load (lbf)	Extension at Maximum Comp. load (in)
1	0001	3600.84	-0.0311
2	0002	3602.08	-0.0325
3	0003	3544.59	-0.0320
4	0004	3585.56	-0.0325
5	0005	3569.33	-0.0320

Cherry Aerospace Compression Tests WOID 88040122 520 C, 4 Hrs

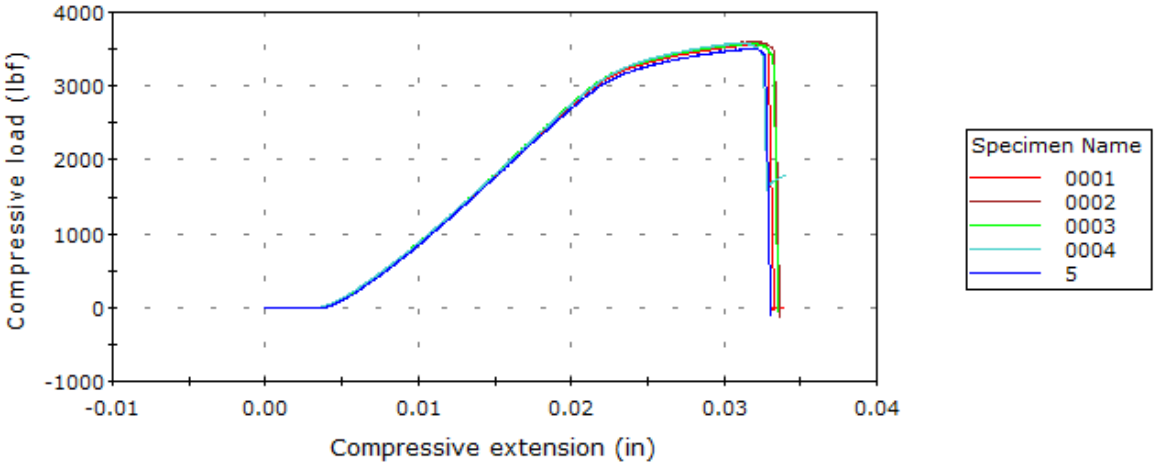

520	Specimen label	Maximum Load (lbf)	Extension at Maximum Comp. load (in)
1	0001	3567.87	-0.0320
2	0002	3604.96	-0.0320
3	0003	3581.21	-0.0315
4	0004	3583.37	-0.0311
5	0005	3508.61	-0.0320

Cherry Aerospace Compression Tests WOID 88040122 530 C, 4 Hrs

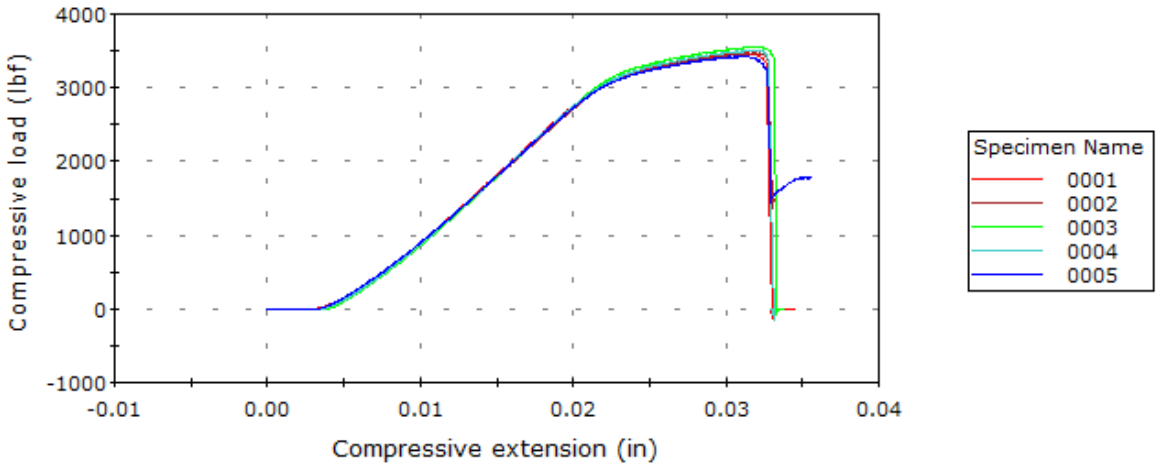

530	Specimen label	Maximum Load (lbf)	Extension at Maximum Comp. load (in)
1	0001	3474.86	-0.0315
2	0002	3474.98	-0.0320
3	0003	3557.32	-0.0320
4	0004	3510.87	-0.0320
5	0005	3431.59	-0.0311

Cherry Aerospace Compression Tests WOID 88040122 Heat Treated 540 C, 4 Hrs

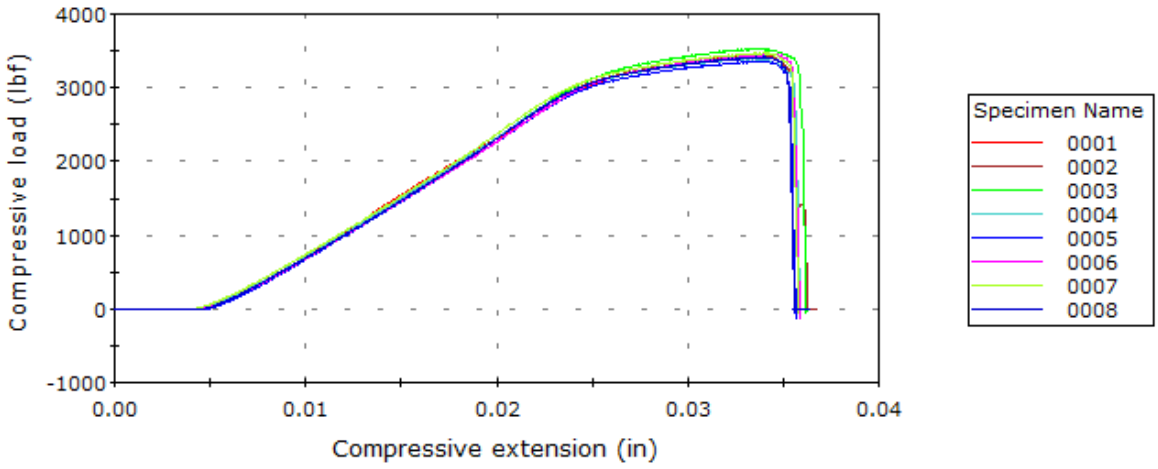

540	Specimen label	Maximum Load (lbf)	Extension at Maximum Comp. load (in)
1	0001	3448.05	-0.0335
2	0002	3439.78	-0.0335
3	0003	3530.99	-0.0335
4	0004	3401.49	-0.0335
5	0005	3363.95	-0.0340
6	0006	3454.10	-0.0345
7	0007	3474.65	-0.0340
8	0008	3417.92	-0.0340

Cherry Aerospace Compression Tests WOID 88040122 Heat Treated 550 C, 4 Hrs

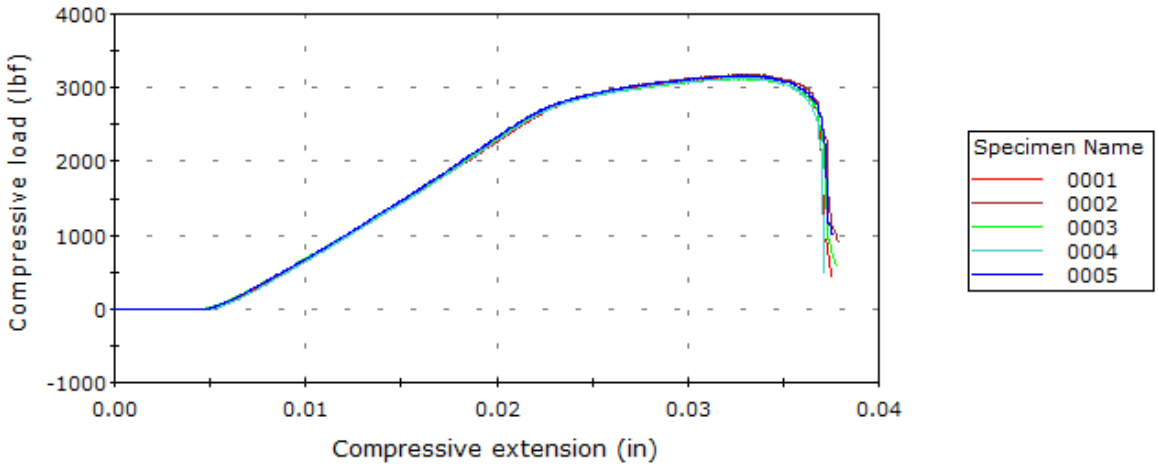

550	Specimen label	Maximum Load (lbf)	Extension at Maximum Comp. load (in)
1	0001	3159.30	-0.0331
2	0002	3181.20	-0.0331
3	0003	3127.56	-0.0326
4	0004	3135.53	-0.0331
5	0005	3169.84	-0.0326

Cherry Aerospace Compression Tests WOID 88040122 Heat Treated 560 C, 4 Hrs

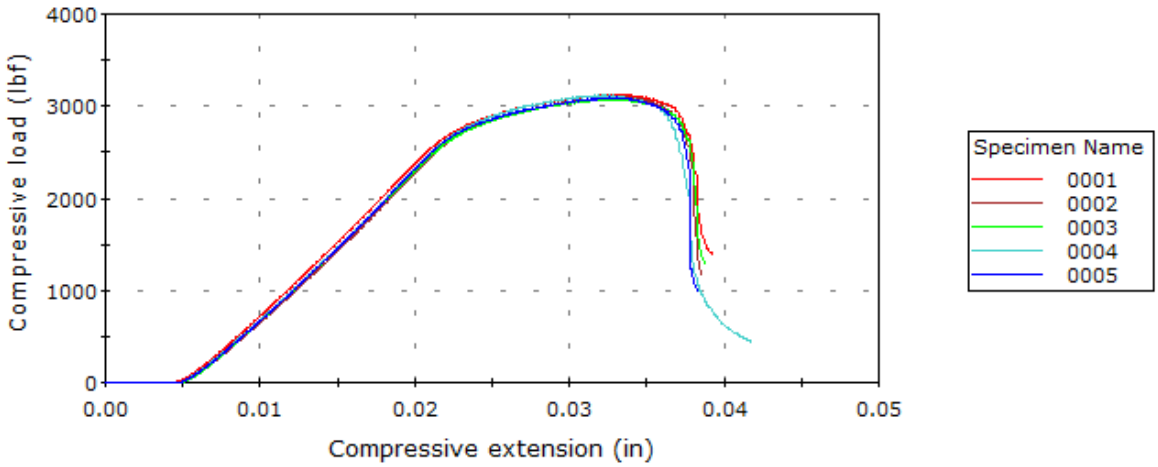

560	Specimen label	Maximum Load (lbf)	Extension at Maximum Comp. load (in)
1	0001	3132.20	-0.0331
2	0002	3107.14	-0.0331
3	0003	3082.26	-0.0326
4	0004	3123.81	-0.0321
5	0005	3096.26	-0.0326

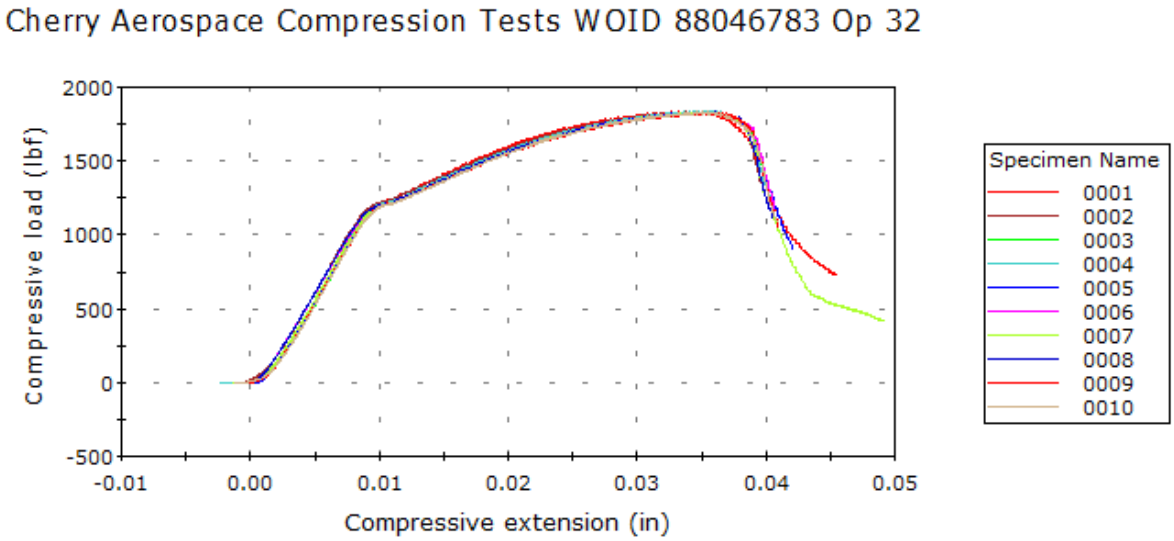

32	Specimen label	Maximum Load (lbf)	Extension at Maximum Comp. load (in)
1	0001	1836.91	-0.0346
2	0002	1839.68	-0.0351
3	0003	1831.99	-0.0355
4	0004	1840.68	-0.0351
5	0005	1834.19	-0.0351
6	0006	1832.76	-0.0355
7	0007	1832.75	-0.0351
8	0008	1833.75	-0.0360
9	0009	1830.92	-0.0360
10	0010	1833.40	-0.0351

Cherry Aerospace Compression Tests WOID 88046783 OP 71

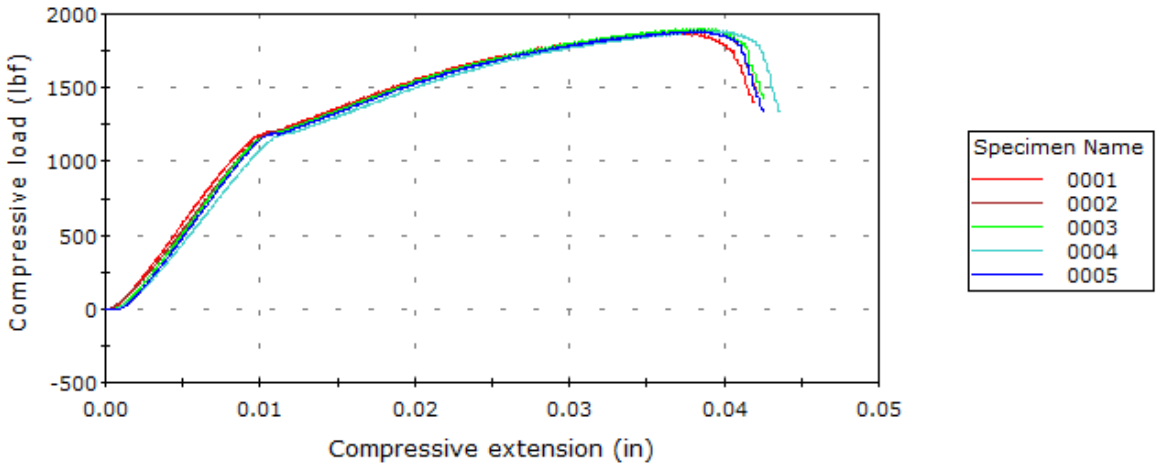

71	Specimen label	Maximum Load (lbf)	Extension at Maximum Comp. load (in)
1	0001	1871.79	-0.0369
2	0002	1894.76	-0.0383
3	0003	1904.98	-0.0383
4	0004	1890.60	-0.0397
5	0005	1887.50	-0.0383

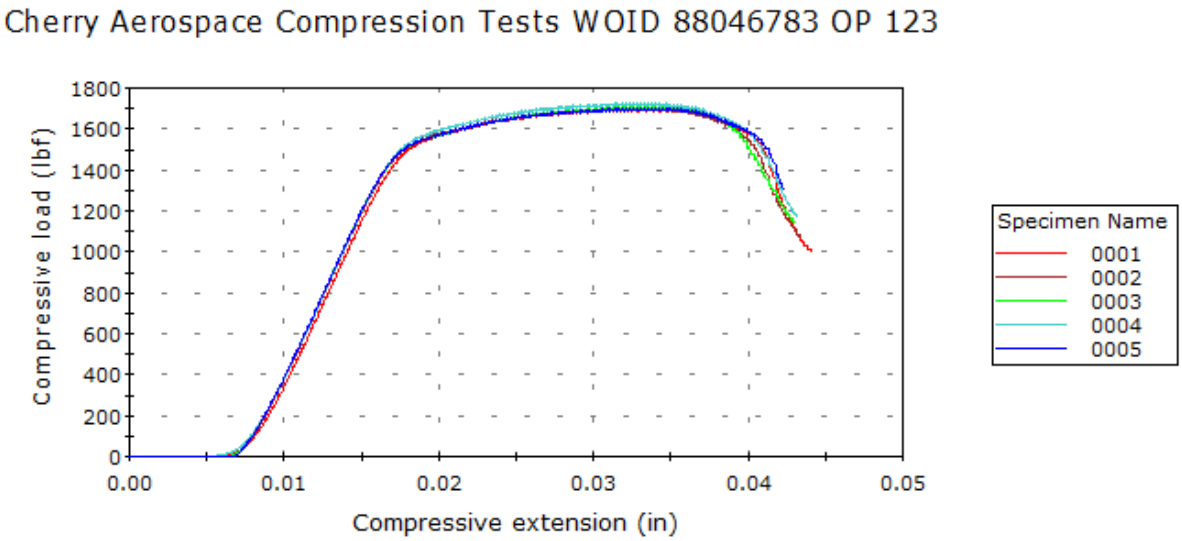

123	Specimen label	Maximum Load (lbf)	Extension at Maximum Comp. load (in)
1	0001	1700.71	-0.0333
2	0002	1703.78	-0.0333
3	0003	1713.41	-0.0338
4	0004	1729.18	-0.0333
5	0005	1704.91	-0.0338

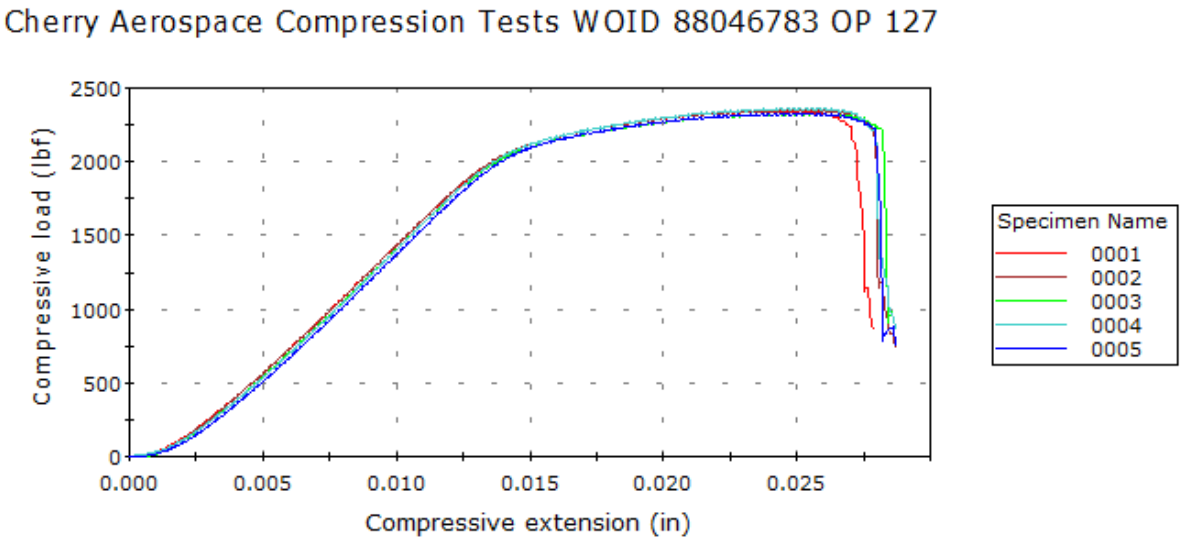

127	Specimen label	Maximum Load (lbf)	Extension at Maximum Comp. load (in)
1	0001	2350.72	-0.0242
2	0002	2356.34	-0.0252
3	0003	2329.40	-0.0252
4	0004	2365.47	-0.0256
5	0005	2331.03	-0.0256

Cherry Aerospace Compression Tests WOID 88046783 Heat Treated 510 C 1.5 Hours

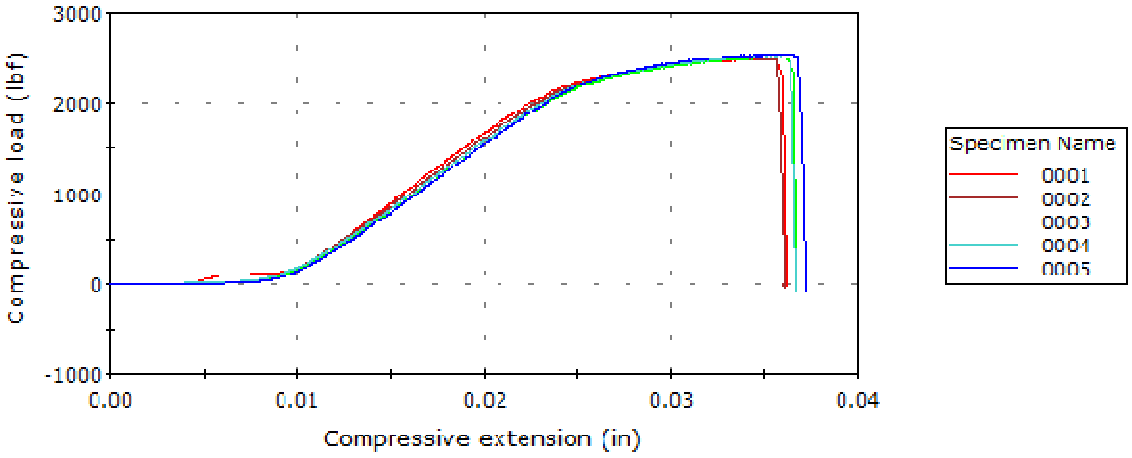

510	Specimen label	Maximum Load (lbf)	Extension at Maximum Comp. load (in)
1	0001	2487.88	-0.0343
2	0002	2499.95	-0.0347
3	0003	2507.04	-0.0357
4	0004	2518.64	-0.0352
5	0005	2547.96	-0.0361

Cherry Aerospace Compression Tests WOID 88046783 Heat Treated 520 C 4 Hours

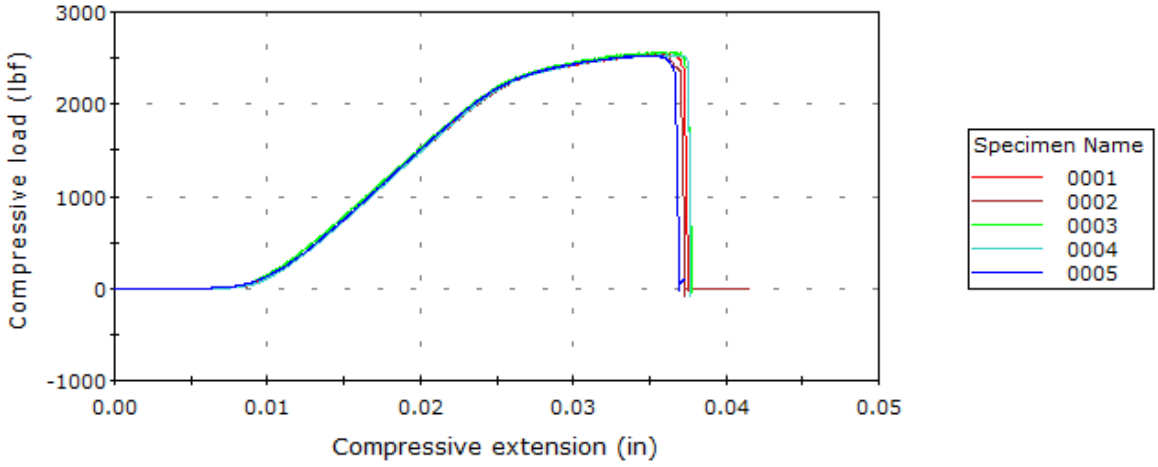

520	Specimen label	Maximum Load (lbf)	Extension at Maximum Comp. load (in)
1	0001	2541.19	-0.0361
2	0002	2550.39	-0.0357
3	0003	2563.35	-0.0361
4	0004	2534.42	-0.0366
5	0005	2531.96	-0.0352

Cherry Aerospace Compression Tests WOID 88046783 Heat Treated 530 C 4 Hours

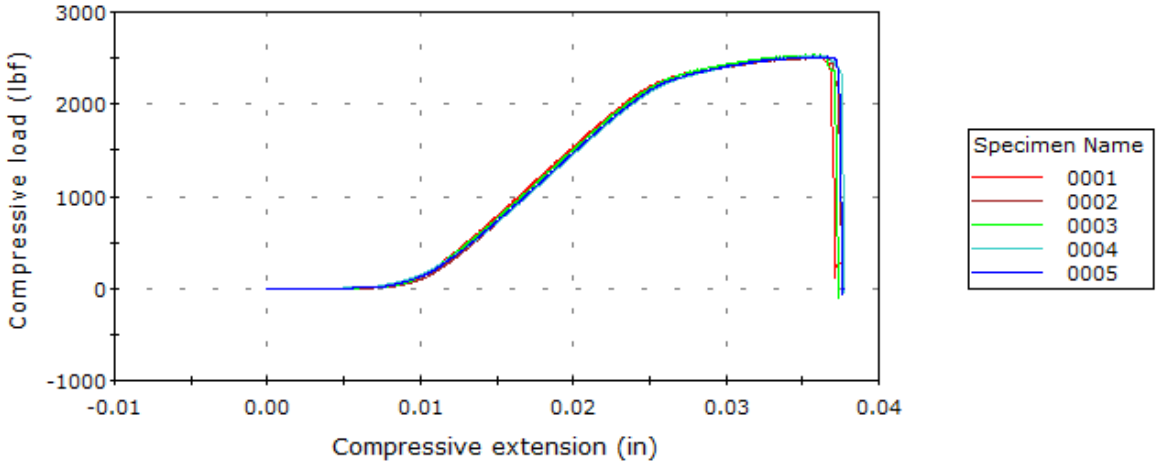

530	Specimen label	Maximum Load (lbf)	Extension at Maximum Comp. load (in)
1	0001	2535.47	-0.0357
2	0002	2507.55	-0.0361
3	0003	2534.78	-0.0361
4	0004	2524.84	-0.0361
5	0005	2514.29	-0.0361

Cherry Aerospace Compression Tests WOID 88046783 Heat Treated 540 C 4 Hours

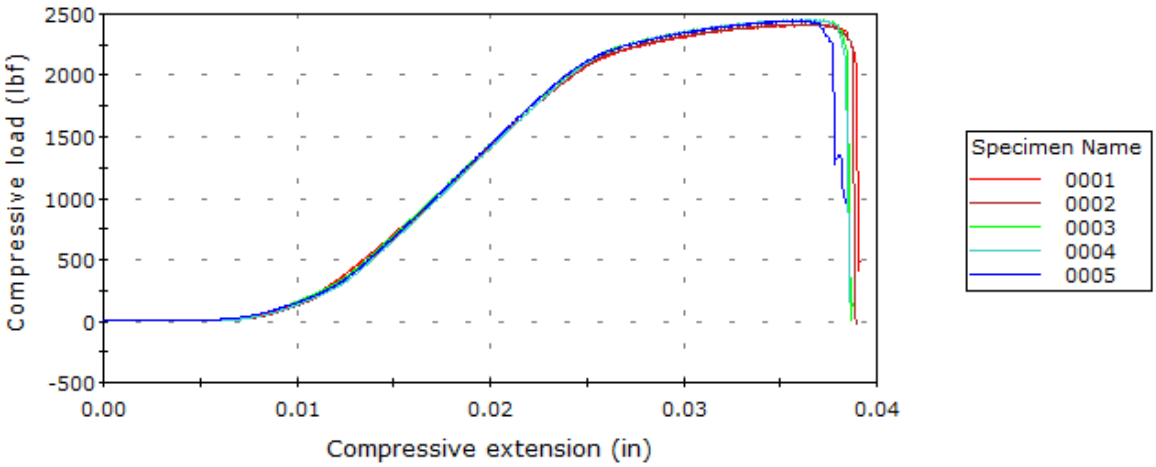

540	Specimen label	Maximum Load (lbf)	Extension at Maximum Comp. load (in)
1	0001	2418.89	-0.0371
2	0002	2421.93	-0.0366
3	0003	2455.45	-0.0366
4	0004	2456.82	-0.0366
5	0005	2449.35	-0.0357

Cherry Aerospace Compression Tests WOID 88046783 Heat Treated 550 C 4 Hours

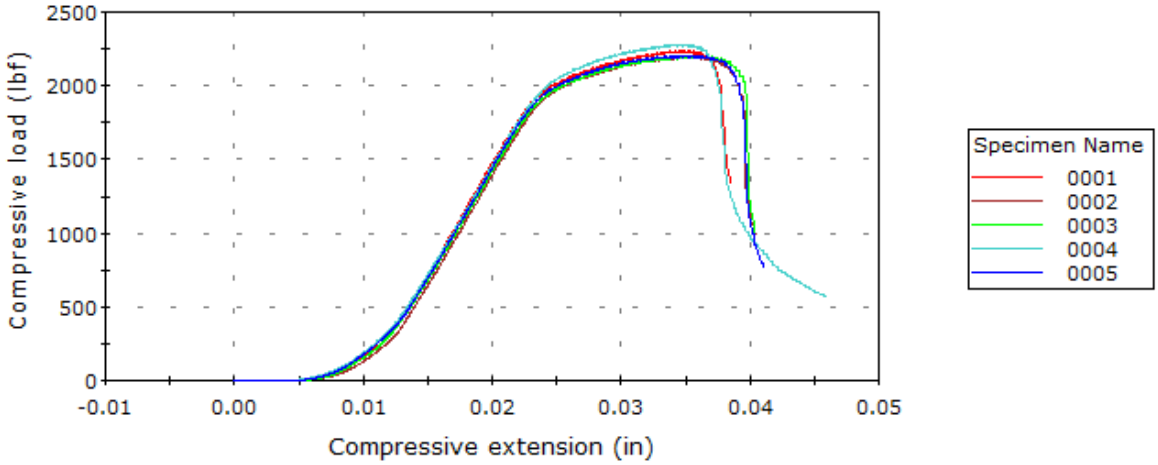

550	Specimen label	Maximum Load (lbf)	Extension at Maximum Comp. load (in)
1	0001	2238.64	-0.0347
2	0002	2197.48	-0.0357
3	0003	2201.11	-0.0366
4	0004	2282.24	-0.0347
5	0005	2206.01	-0.0347

Cherry Aerospace Compression Tests WOID 88046783 Heat Treated 560 C 4 Hours

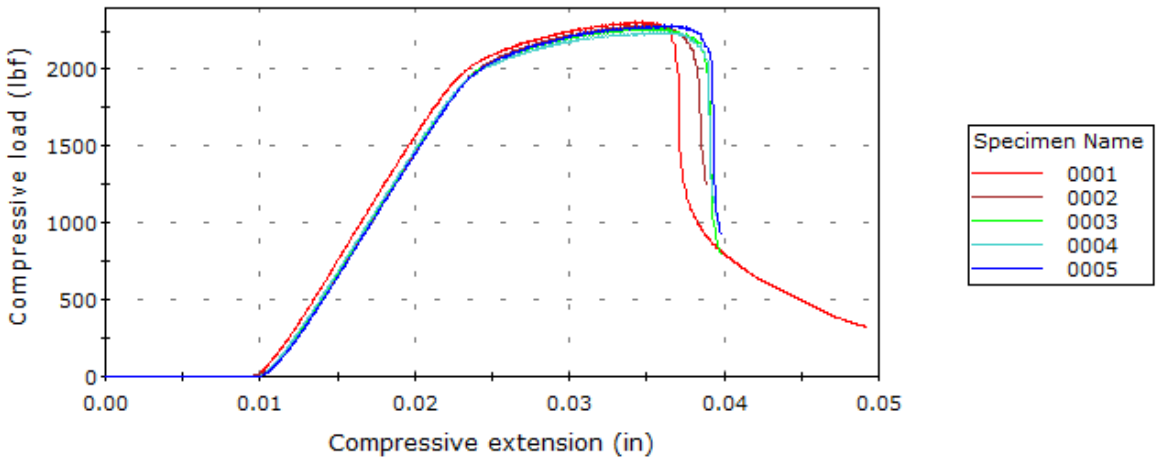

560	Specimen label	Maximum Load (lbf)	Extension at Maximum Comp. load (in)
1	0001	2311.19	-0.0343
2	0002	2290.86	-0.0352
3	0003	2269.99	-0.0357
4	0004	2242.51	-0.0357
5	0005	2287.45	-0.0361

Cherry Aerospace Compression Tests WOID 88047697 OP 32

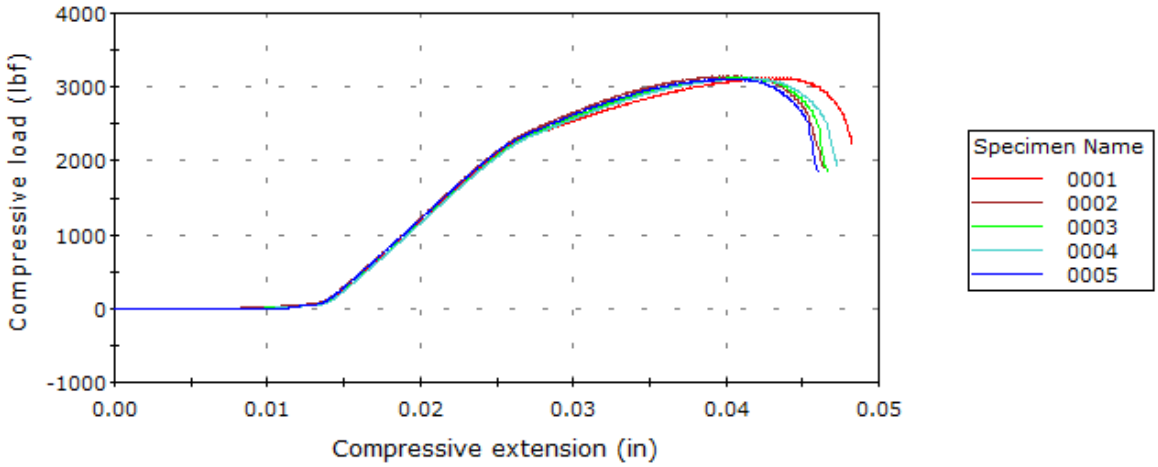

32	Specimen label	Maximum Load (lbf)	Extension at Maximum Comp. load (in)
1	0001	3128.36	-0.0433
2	0002	3150.02	-0.0405
3	0003	3128.33	-0.0414
4	0004	3120.76	-0.0414
5	0005	3113.71	-0.0405

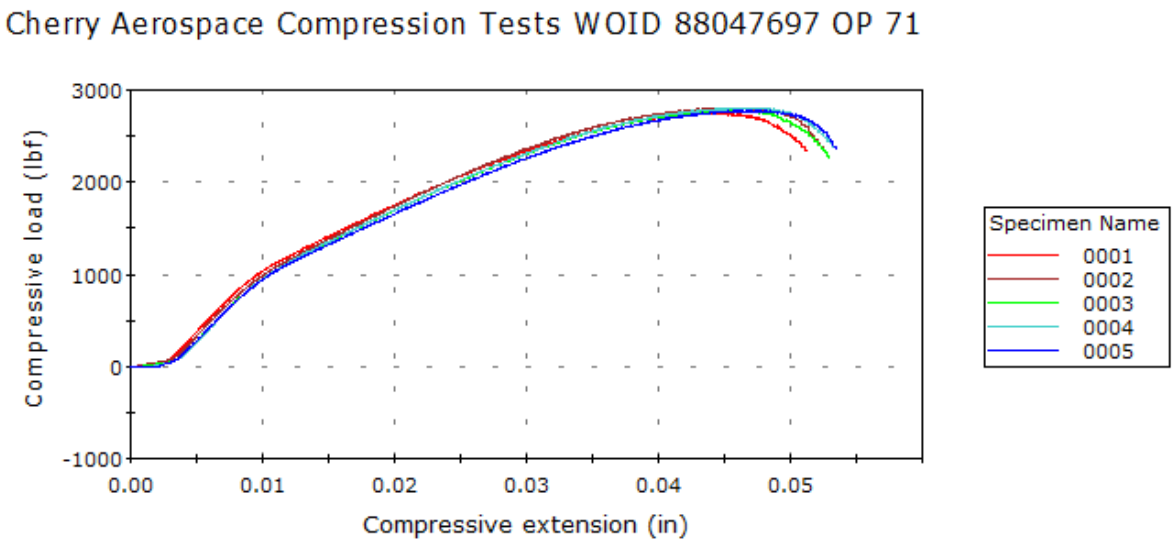

71	Specimen label	Maximum Load (lbf)	Extension at Maximum Comp. load (in)
1	0001	2753.28	-0.0443
2	0002	2809.68	-0.0462
3	0003	2783.58	-0.0462
4	0004	2810.09	-0.0471
5	0005	2782.36	-0.0462

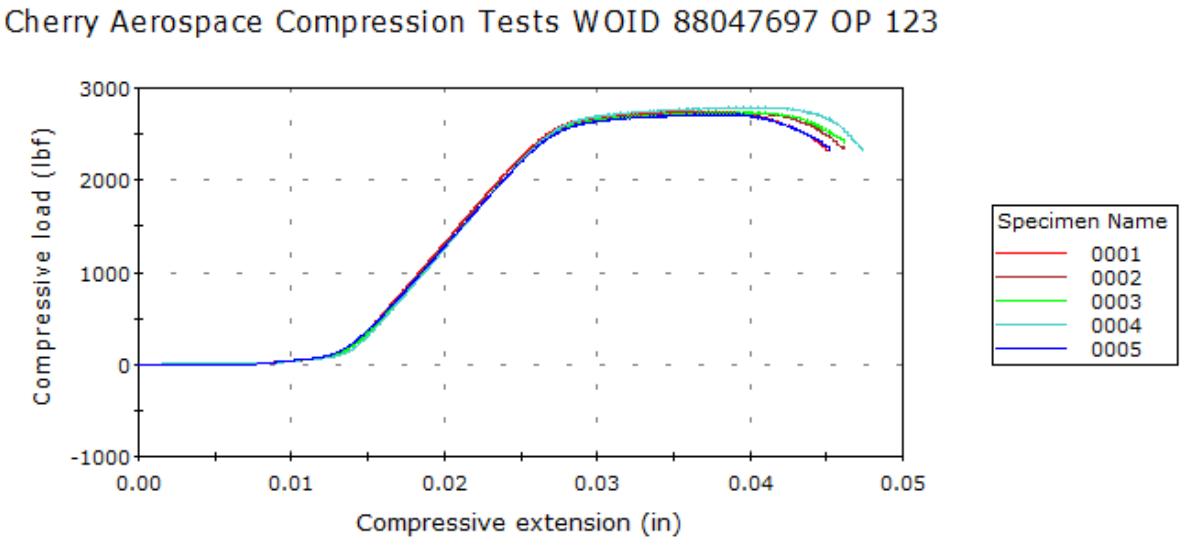

123	Specimen label	Maximum Load (lbf)	Extension at Maximum Comp. load (in)
1	0001	2750.70	-0.0367
2	0002	2741.03	-0.0391
3	0003	2741.02	-0.0391
4	0004	2793.40	-0.0405
5	0005	2720.53	-0.0386

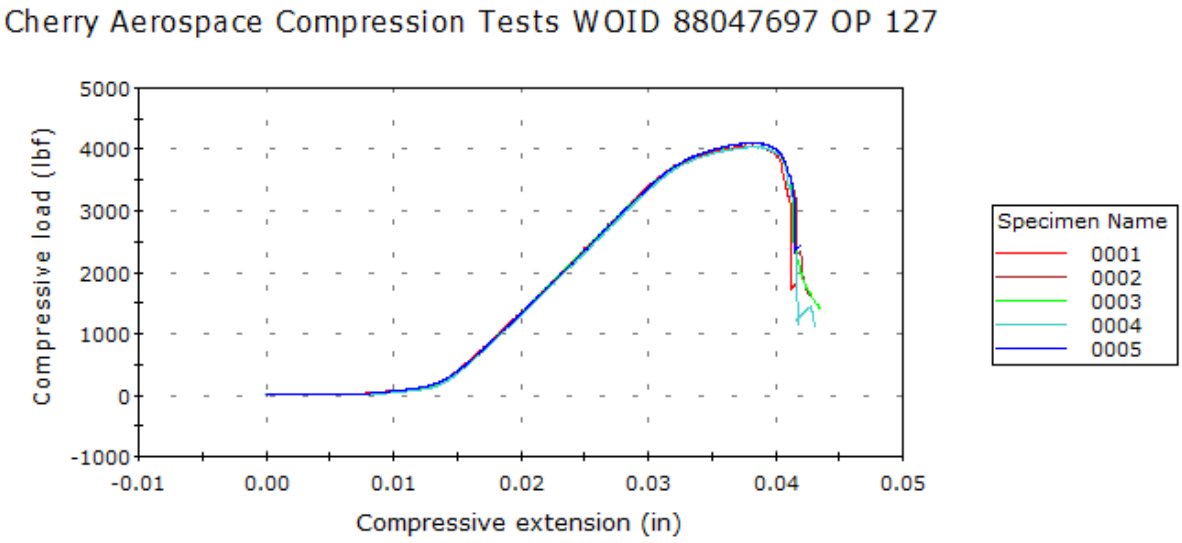

127	Specimen label	Maximum Load (lbf)	Extension at Maximum Comp. load (in)
1	0001	4062.33	-0.0382
2	0002	4049.06	-0.0382
3	0003	4113.16	-0.0382
4	0004	4048.55	-0.0382
5	0005	4112.65	-0.0382

Cherry Aerospace Compression Tests WOID 88047697 Heat Treated 510 °C, 1.5 Hours

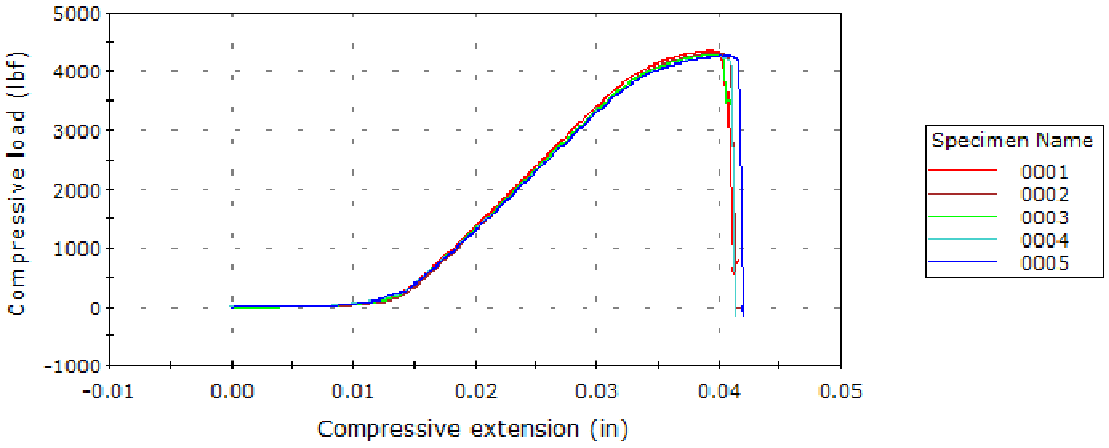

510	Specimen label	Maximum Load (lbf)	Extension at Maximum Comp. load (in)
1	0001	4368.60	-0.0396
2	0002	4325.92	-0.0400
3	0003	4297.79	-0.0396
4	0004	4266.57	-0.0400
5	0005	4280.85	-0.0405

Cherry Aerospace Compression Tests WOID 88047697 Heat Treated 520 °C, 4 Hours

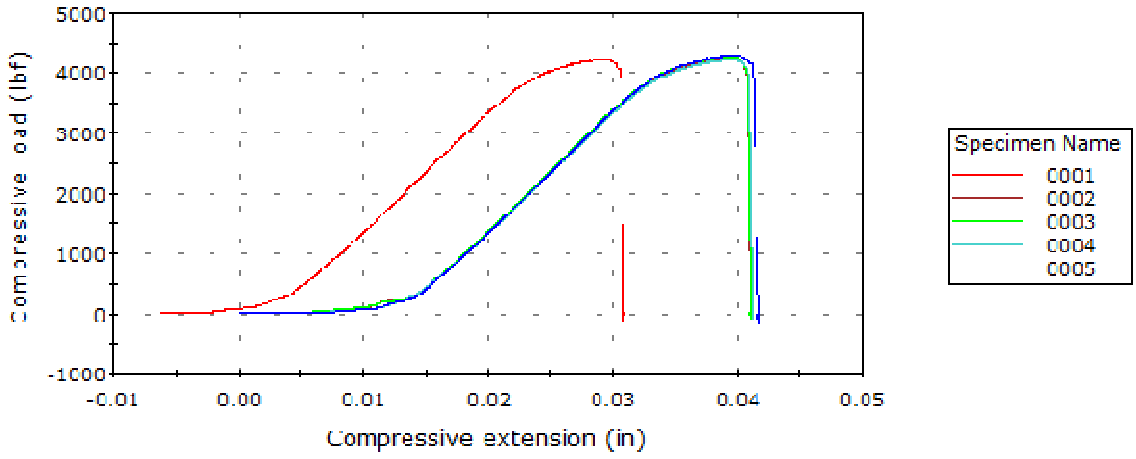

520	Specimen label	Maximum Load (lbf)	Extension at Maximum Comp. load (in)
1	0001	4235.45	-0.0296
2	0002	4251.70	-0.0396
3	0003	4274.26	-0.0391
4	0004	4236.01	-0.0396
5	0005	4292.79	-0.0396

Cherry Aerospace Compression Tests WOID 88017697 Heat Treated 530 °C, 4 Hours

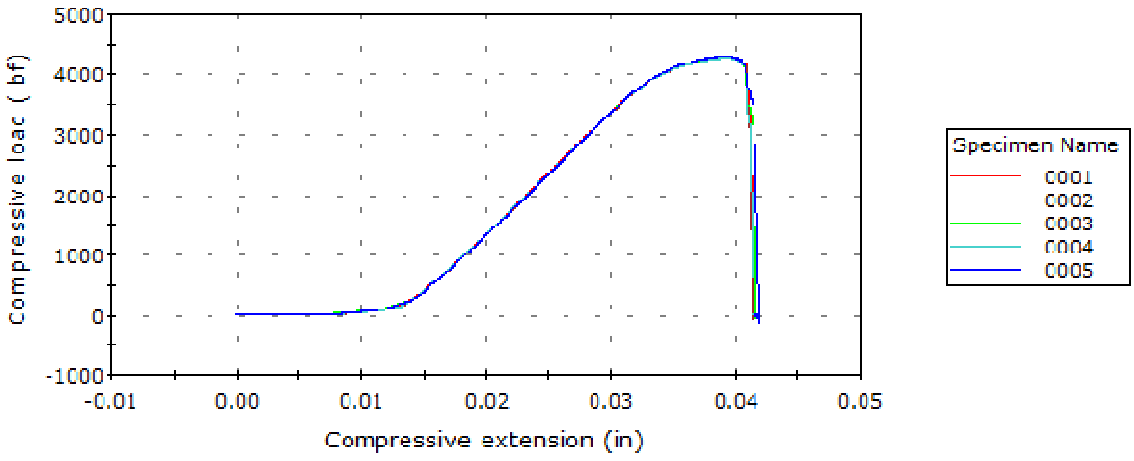

530	Specimen label	Maximum Load (lbf)	Extension at Maximum Comp. load (in)
1	0001	4294.28	-0.0396
2	0002	4297.95	-0.0396
3	0003	4301.72	-0.0391
4	0004	4290.36	-0.0396
5	0005	4321.49	-0.0391

Cherry Aerospace Compression Tests WOID 88047697 Heat Treated 540 °C, 4 Hours

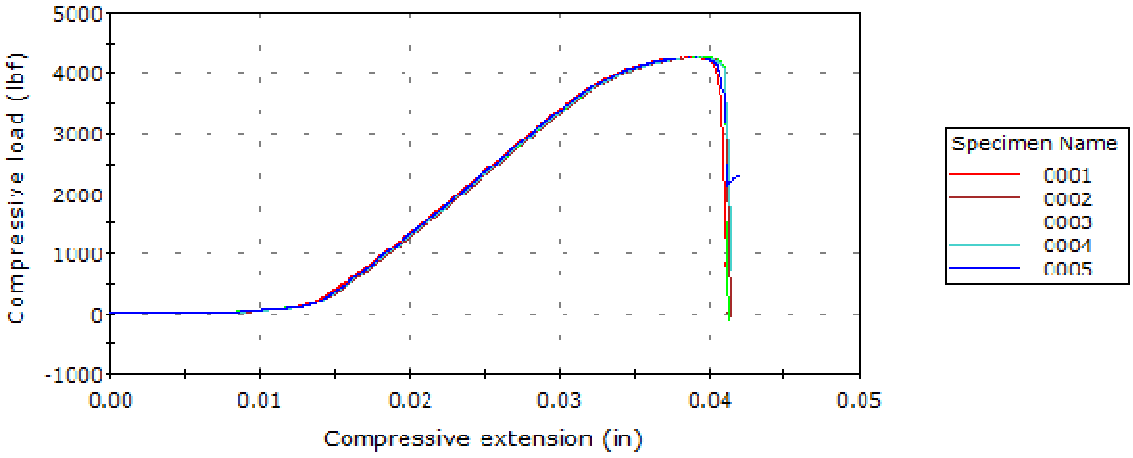

540	Specimen label	Maximum Load (lbf)	Extension at Maximum Comp. load (in)
1	0001	4286.15	-0.0391
2	0002	4276.73	-0.0396
3	0003	4292.44	-0.0396
4	0004	4276.07	-0.0396
5	0005	4275.40	-0.0391

Cherry Aerospace Compression Tests WOID 88047697 Heat Treated 550 °C, 4 Hours

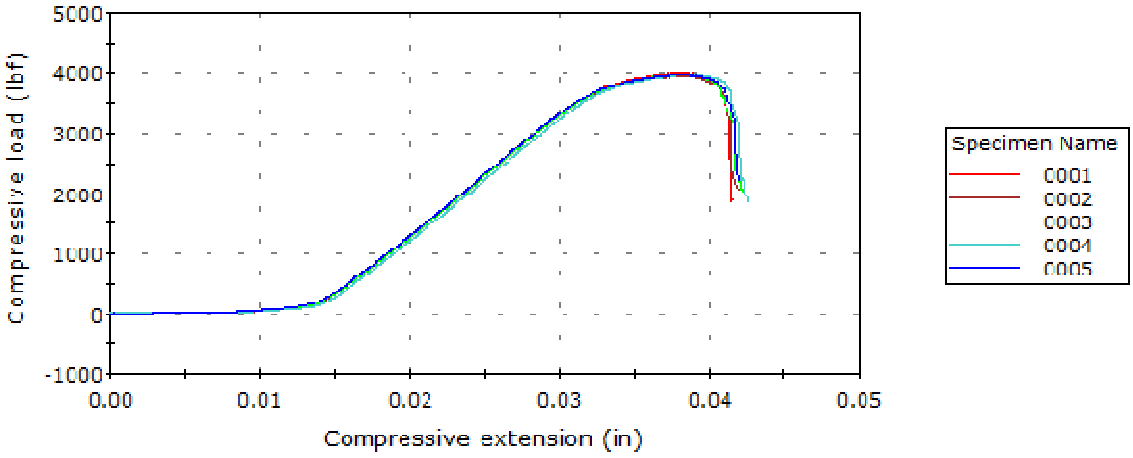

550	Specimen label	Maximum Load (lbf)	Extension at Maximum Comp. load (in)
1	0001	4019.40	-0.0382
2	0002	3966.85	-0.0382
3	0003	3995.20	-0.0382
4	0004	3994.27	-0.0386
5	0005	3990.53	-0.0382

Cherry Aerospace Compression Tests WOID 88047697 Heat Treated 560 °C, 4 Hours

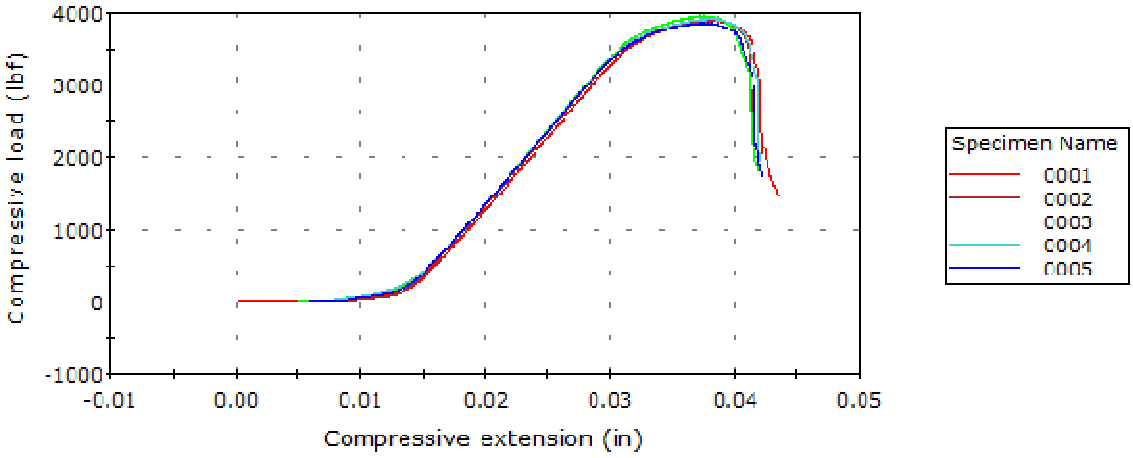

560	Specimen label	Maximum Load (lbf)	Extension at Maximum Comp. load (in)
1	0001	3902.58	-0.0386
2	0002	3916.73	-0.0382
3	0003	3967.96	-0.0377
4	0004	3927.40	-0.0382
5	0005	3869.82	-0.0377

Cherry Aerospace Compression Tests WOID 88030569 EDS 3635-06-07 FIRST 11/33

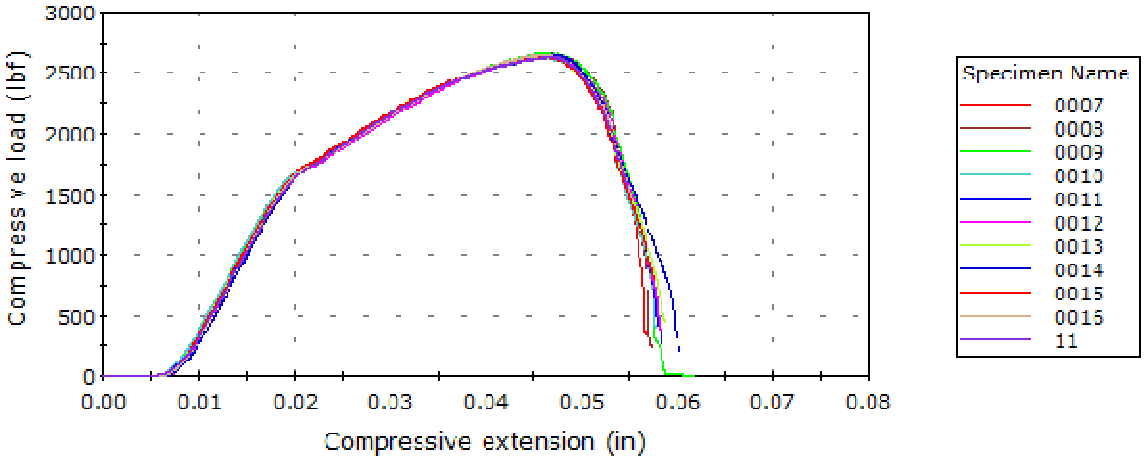

Cherry Aerospace Compression Tests WOID 88030569 EDS 3635-06-07 SECOND 22/33

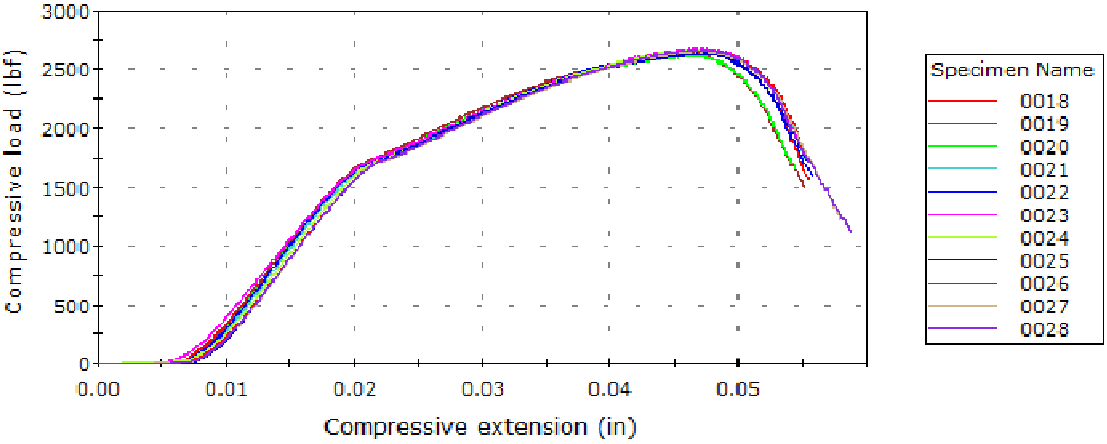

Cherry Aerospace Compression Tests WOID 88030560 EDS 3635-06-07 THIRD 33/33

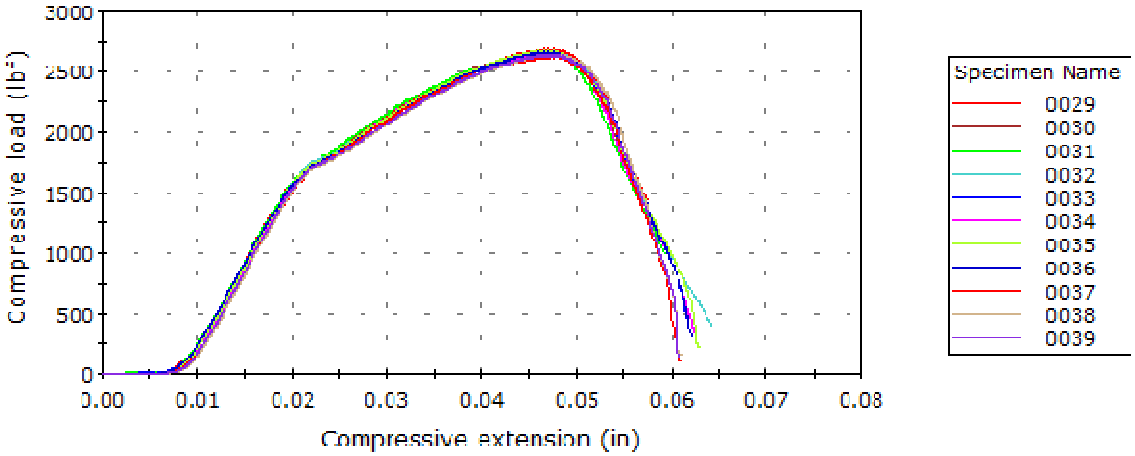

32	Specimen label	Maximum Load (lbf)	Extension at Maximum Comp. load (in)
1	0007	2632.84	-0.0462
2	0008	2657.05	-0.0466
3	0009	2661.86	-0.0466
4	0010	2635.46	-0.0457
5	0011	2631.45	-0.0466
6	0012	2637.93	-0.0462
7	0013	2625.90	-0.0462
8	0014	2650.49	-0.0471
9	0015	2632.40	-0.0462
10	0016	2647.55	-0.0462
11		2633.01	-0.0471

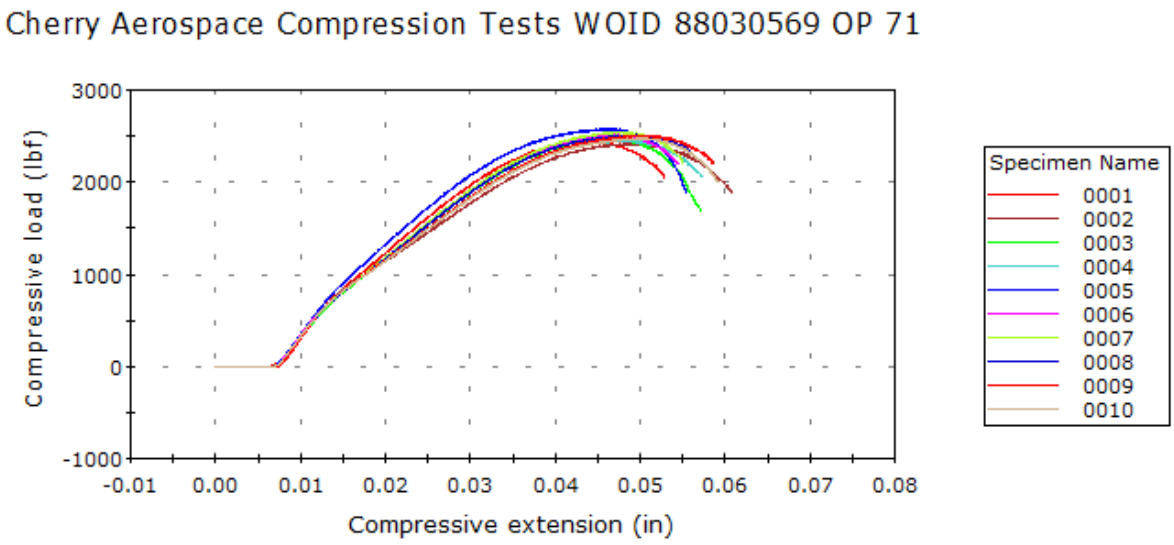

OP 71	Specimen label	Maximum Load (lbf)	Extension at Maximum Comp. load (in)
1	0001	2445.61	-0.0439
2	0002	2418.89	-0.0495
3	0003	2479.58	-0.0467
4	0004	2454.04	-0.0486
5	0005	2581.09	-0.0462
6	0006	2518.78	-0.0467
7	0007	2545.67	-0.0476
8	0008	2513.99	-0.0495
9	0009	2509.77	-0.0500
10	0010	2480.10	-0.0500

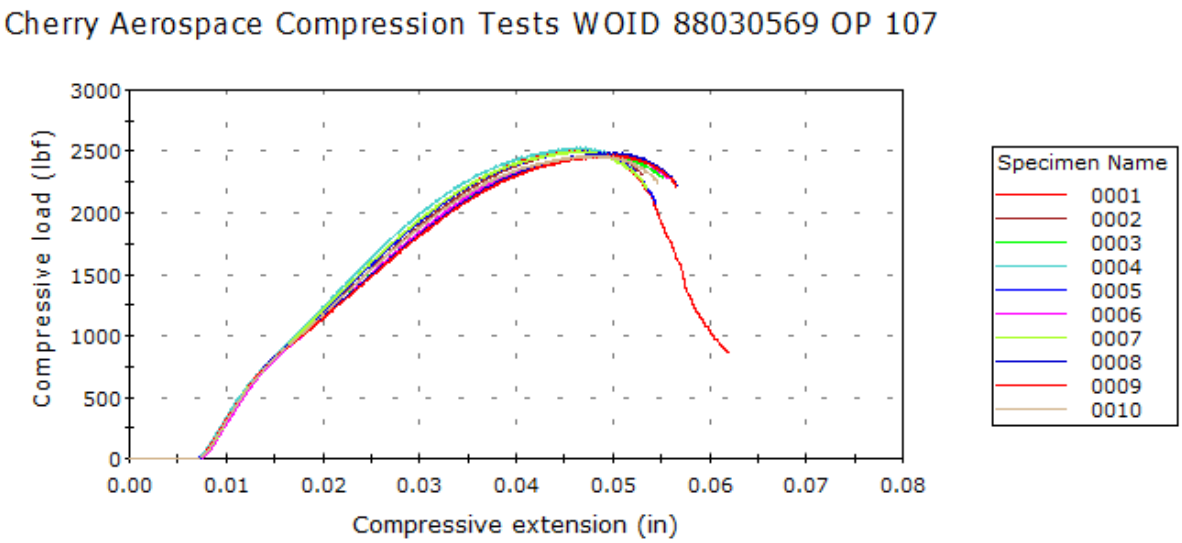

107	Specimen label	Maximum Load (lbf)	Extension at Maximum Comp. load (in)
1	0001	2509.94	-0.0467
2	0002	2512.28	-0.0476
3	0003	2475.02	-0.0495
4	0004	2531.47	-0.0467
5	0005	2506.33	-0.0467
6	0006	2482.70	-0.0495
7	0007	2505.28	-0.0467
8	0008	2491.77	-0.0500
9	0009	2472.57	-0.0500
10	0010	2467.83	-0.0486

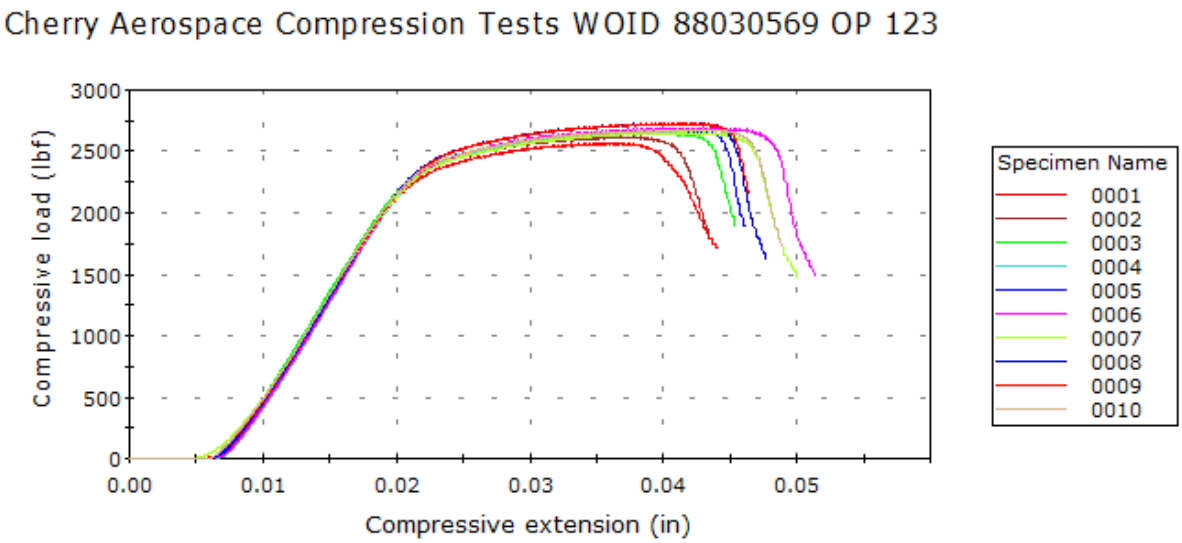

123	Specimen label	Maximum Load (lbf)	Extension at Maximum Comp. load (in)
1	0001	2571.00	-0.0369
2	0002	2623.03	-0.0373
3	0003	2653.23	-0.0387
4	0004	2665.72	-0.0415
5	0005	2678.96	-0.0387
6	0006	2694.21	-0.0429
7	0007	2657.57	-0.0415
8	0008	2734.46	-0.0415
9	0009	2734.78	-0.0415
10	0010	2683.23	-0.0425

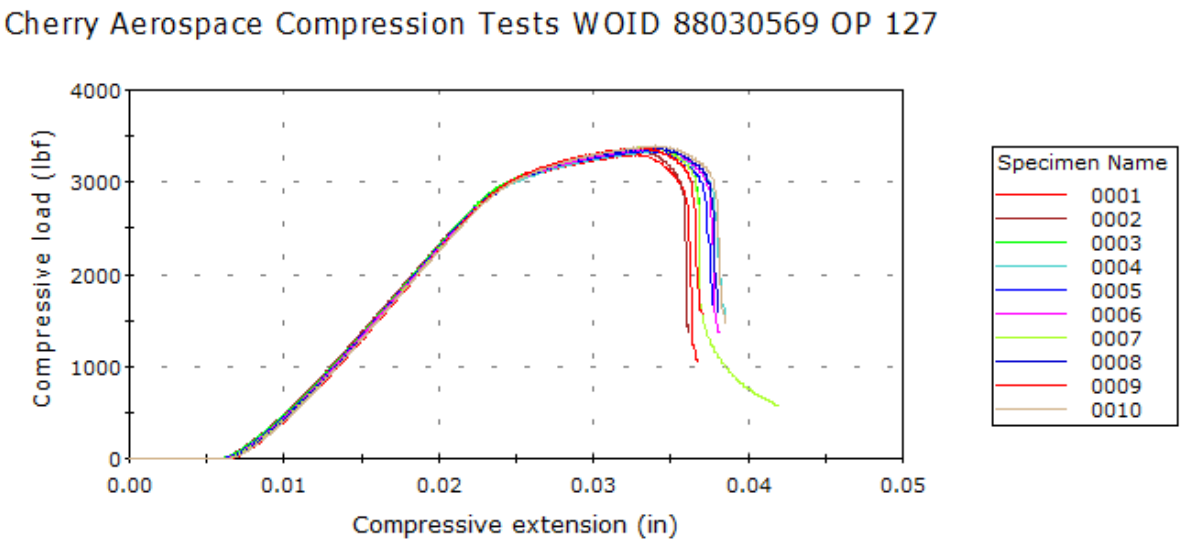

127	Specimen label	Maximum Load (lbf)	Extension at Maximum Comp. load (in)
1	0001	3303.46	-0.0326
2	0002	3340.55	-0.0331
3	0003	3391.55	-0.0336
4	0004	3335.32	-0.0340
5	0005	3347.43	-0.0336
6	0006	3374.96	-0.0340
7	0007	3389.49	-0.0336
8	0008	3376.62	-0.0336
9	0009	3377.88	-0.0331
10	0010	3394.16	-0.0340

Cherry Aerospace Compression Tests WOID 88030569 Heat Treated 510C 1.5 hours

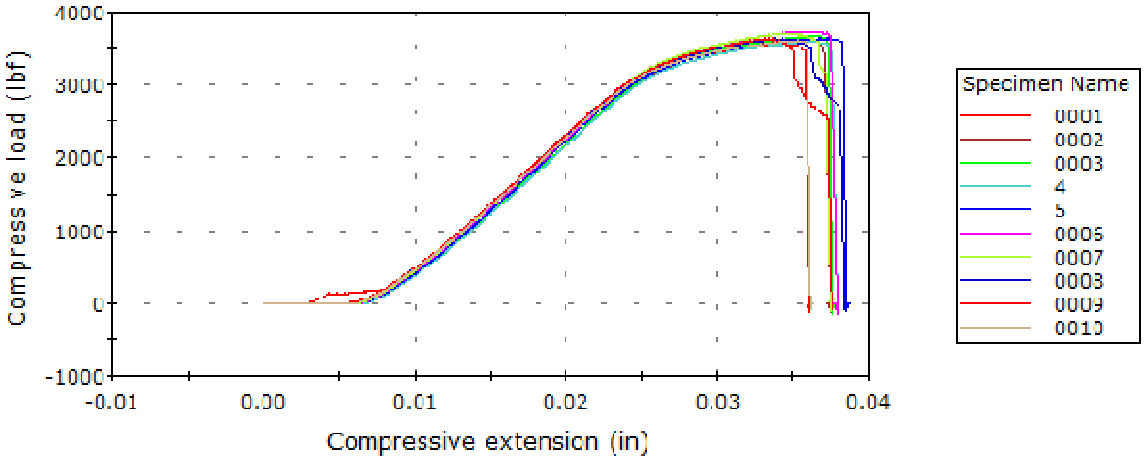

510	Specimen label	Maximum Load (lbf)	Extension at Maximum Comp. load (in)
1	0001	3578.79	-0.0348
2	0002	3645.27	-0.0358
3	0003	3677.02	-0.0363
4	0004	3604.51	-0.0363
5	0005	3644.07	-0.0367
6	0006	3736.39	-0.0363
7	0007	3713.08	-0.0348
8	0008	3641.71	-0.0339
9	0009	3646.84	-0.0334
10	0010	3615.64	-0.0353

Cherry Aerospace Compression Tests WOID 88030569 Heat Treated 520C 4 hours

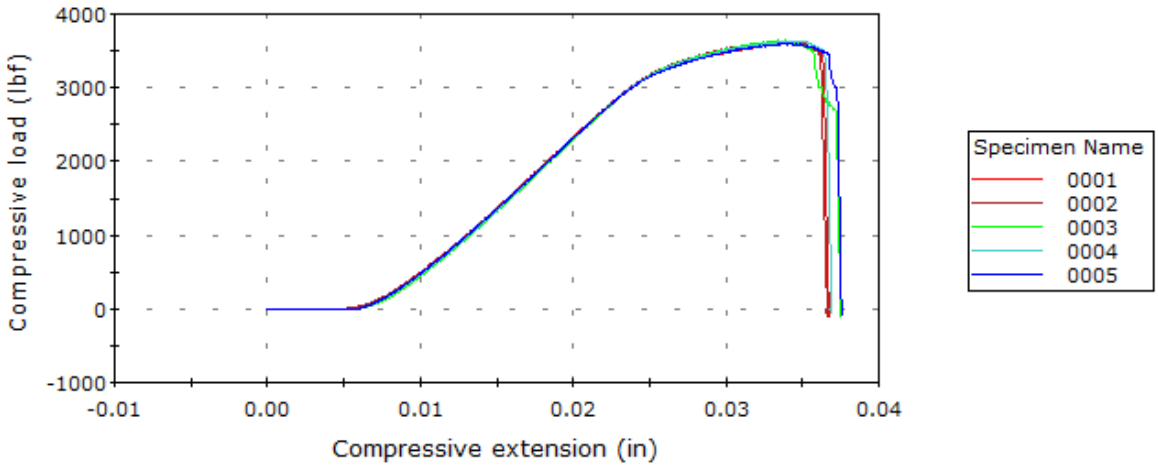

520	Specimen label	Maximum Load (lbf)	Extension at Maximum Comp. load (in)
1	0001	3622.58	-0.0348
2	0002	3640.94	-0.0339
3	0003	3641.64	-0.0339
4	0004	3638.90	-0.0344
5	0005	3603.53	-0.0339

Cherry Aerospace Compression Tests WOID 88030569 530 C, 4 Hrs

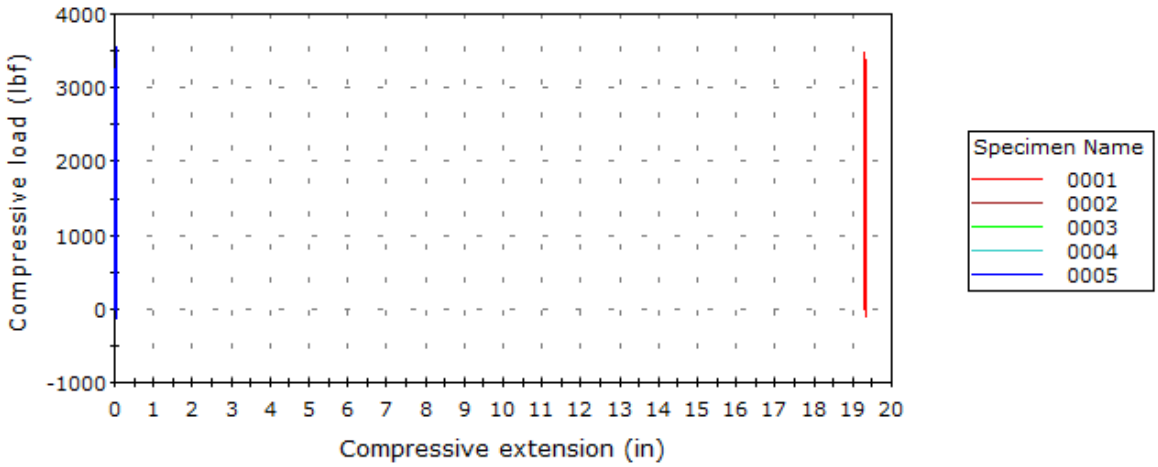

530	Specimen label	Maximum Load (lbf)	Extension at Maximum Comp. load (in)
1	0001	3483.62	-19.3143
2	0002	3516.04	-0.0330
3	0003	3501.05	-0.0315
4	0004	3541.54	-0.0311
5	0005	3555.02	-0.0311

Cherry Aerospace Compression Tests WOID 88030569 540 C, 4 Hrs

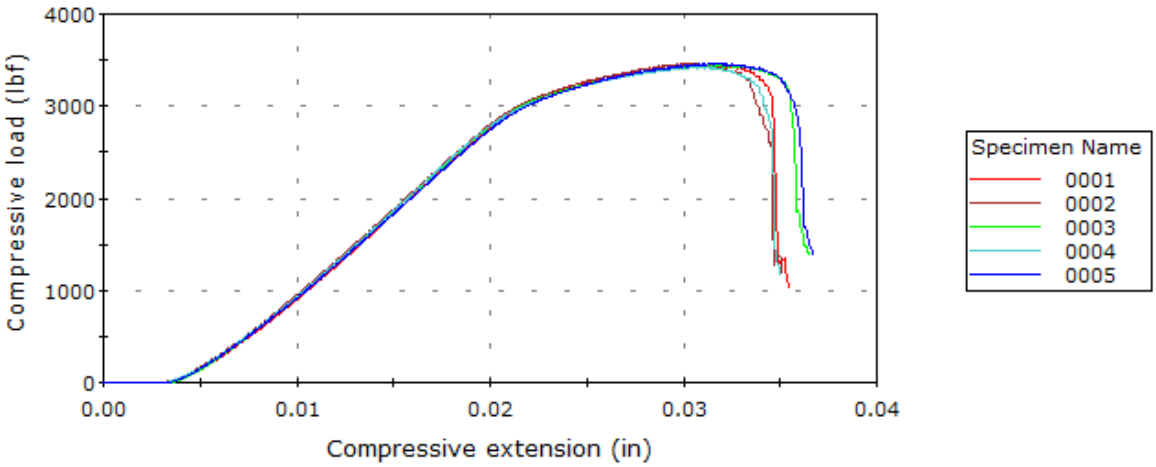

540	Specimen label	Maximum Load (lbf)	Extension at Maximum Comp. load (in)
1	0001	3458.19	-0.0311
2	0002	3467.24	-0.0306
3	0003	3444.49	-0.0315
4	0004	3428.22	-0.0311
5	0005	3466.03	-0.0315

Cherry Aerospace Compression Tests WOID 88030569 550 C, 4 Hrs

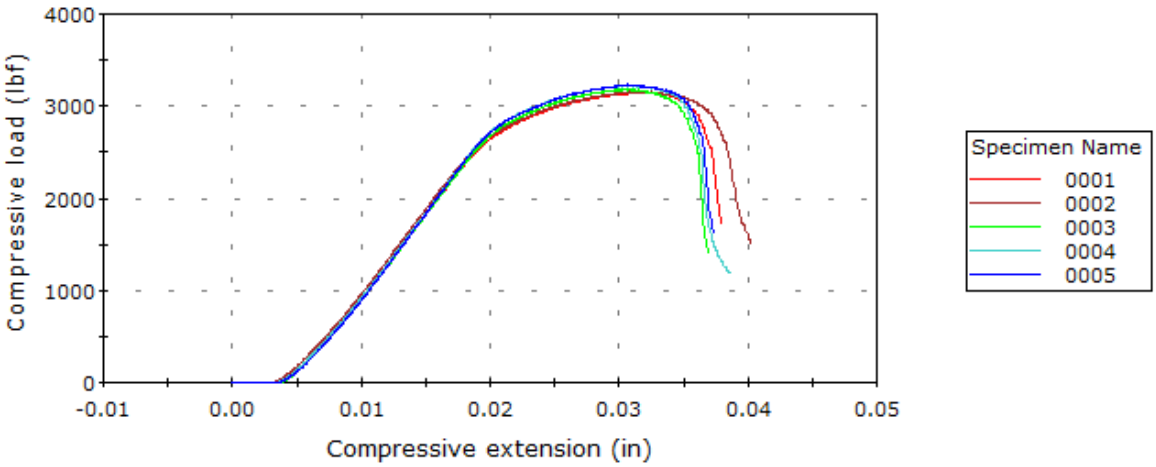

550	Specimen label	Maximum Load (lbf)	Extension at Maximum Comp. load (in)
1	0001	3155.82	-0.0315
2	0002	3163.31	-0.0315
3	0003	3187.87	-0.0306
4	0004	3229.48	-0.0306
5	0005	3234.50	-0.0306

Cherry Aerospace Compression Tests WOID 88030569 560 C, 4 Hrs

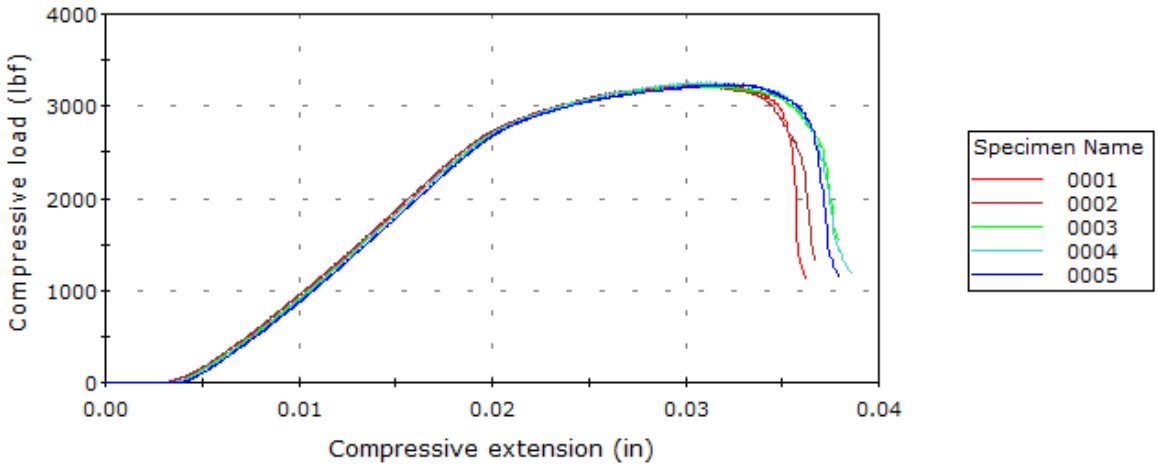

560	Specimen label	Maximum Load (lbf)	Extension at Maximum Comp. load (in)
1	0001	3249.12	-0.0311
2	0002	3237.34	-0.0301
3	0003	3221.75	-0.0311
4	0004	3257.89	-0.0306
5	0005	3237.74	-0.0325